# Moments and Moment Invariants

# in Image Analysis

Jan Flusser, Barbara Zitová,
and Tomáš Suk

**Institute of Information Theory and Automation**
Prague, Czech Republic

## Problem formulation

**Non-ideal imaging conditions → degradation of the image**

$$g = D(f)$$

***D*** **- unknown degradation operator**

## Basic approaches

- **Brute force**
- **Normalized position → inverse problem**
- **Description of the objects by invariants**

## What are invariants?

**Invariants are functionals defined on the image space such that**

- $I(f) = I(D(f))$ **for all admissible** $D$
- $I(f_1)$, $I(f_2)$ **"different enough" for different** $f_1$, $f_2$

# What are moments?

## Moments are “projections” of the image function into a polynomial basis

$f(x, y)$ – piecewise continuous image function defined on bounded $\Omega \subset \mathcal{R} \times \mathcal{R}$

$\{\mathcal{P}_{pq}(x, y)\}$ – set of polynomials defined on $\Omega$

$$M_{pq} = \int\int \mathcal{P}_{pq}(x, y) f(x, y) dx dy$$

# Common types of moments

## Geometric moments

$$m_{pq}^{(f)} = \int_{R^2} x^p y^q f(x, y) dx dy$$

## Central moments

$$\mu_{pq}^{(f)} = \int_{R^2} (x - x_t)^p (y - y_t)^q f(x, y) dx dy$$

$$\mu_{pq} = \sum_{k=0}^{p} \sum_{j=0}^{q} \binom{p}{k} \binom{q}{j} (-1)^{k+j} x_t^k y_t^j m_{p-k,q-j}$$

## Common types of moments

### Geometric moments

$$m_{pq}^{(f)} = \int_{R^2} x^p y^q f(x,y) dx dy$$

**Uniqueness theorem**

If $f(x,y)$ is piecewise continuous and $\Omega$ is bounded then

$$f(x,y) \Longleftrightarrow \{m_{pq}\} \quad p,q = 0,1,2,\cdots,\infty$$

# What are moment invariants?

**Functions of moments, invariant to certain class of image degradations**

- **Rotation, translation, scaling**
- **Convolution/blurring**
- **Affine transform**
- **Combined invariants**

# Invariants to translation and scaling

**Normalized central moments**

$$\nu_{pq} = \frac{\mu_{pq}}{\mu_{00}^{w}} \qquad w = \frac{p+q}{2} + 1$$

# Invariants to rotation

## M.K. Hu, 1962 - 7 invariants of 3rd order

$$\phi_1 = \mu_{20} + \mu_{02}$$

$$\phi_2 = (\mu_{20} - \mu_{02})^2 + 4\mu_{11}^2$$

$$\phi_3 = (\mu_{30} - 3\mu_{12})^2 + (3\mu_{21} - \mu_{03})^2$$

$$\phi_4 = (\mu_{30} + \mu_{12})^2 + (\mu_{21} + \mu_{03})^2$$

$$\begin{aligned}\phi_5 &= (\mu_{30} - 3\mu_{12})(\mu_{30} + \mu_{12})((\mu_{30} + \mu_{12})^2 - 3(\mu_{21} + \mu_{03})^2) \\ &+ (3\mu_{21} - \mu_{03})(\mu_{21} + \mu_{03})(3(\mu_{30} + \mu_{12})^2 - (\mu_{21} + \mu_{03})^2)\end{aligned}$$

$$\begin{aligned}\phi_6 &= (\mu_{20} - \mu_{02})((\mu_{30} + \mu_{12})^2 - (\mu_{21} + \mu_{03})^2) + \\ &\quad 4\mu_{11}(\mu_{30} + \mu_{12})(\mu_{21} + \mu_{03})\end{aligned}$$

$$\begin{aligned}\phi_7 &= (3\mu_{21} - \mu_{03})(\mu_{30} + \mu_{12})((\mu_{30} + \mu_{12})^2 - 3(\mu_{21} + \mu_{03})^2) \\ &- (\mu_{30} - 3\mu_{12})(\mu_{21} + \mu_{03})(3(\mu_{30} + \mu_{12})^2 - (\mu_{21} + \mu_{03})^2)\end{aligned}$$

**Hard to find, easy to prove:**

$$x' = x\cos\theta - y\sin\theta$$

$$y' = x\sin\theta + y\cos\theta$$

$$\mu'_{20} = \cos^2\theta \cdot \mu_{20} + \sin^2\theta \cdot \mu_{02} - \sin 2\theta \cdot \mu_{11}$$

$$\mu'_{02} = \sin^2\theta \cdot \mu_{20} + \cos^2\theta \cdot \mu_{02} + \sin 2\theta \cdot \mu_{11}$$

$$\mu'_{11} = \frac{1}{2}\sin 2\theta \cdot (\mu_{20} - \mu_{02}) + \cos 2\theta \cdot \mu_{11}$$

## Drawbacks of the Hu's invariants

**Dependence**

$$\phi_3 = \frac{\phi_5^2 + \phi_7^2}{\phi_4^3}$$

**Incompleteness**

$$m_{11}^2 = \frac{1}{4}(\phi_2 - (\frac{\phi_6}{\phi_4})^2)$$

**Insufficient number → low discriminability**

# Normalized position to rotation

**Constraints**

$$\mu'_{00} = 1$$
$$\mu'_{11} = 0$$

**Rotation angle**

$$\tan 2\theta = \frac{-2\mu_{11}}{\mu_{20} - \mu_{02}}$$

# Normalized position to rotation

**Ambiguity removing**

$$\mu'_{20} \geq \mu'_{02}$$
$$\mu'_{30} \geq 0$$

## Moments in the normalized position

$$M = \begin{pmatrix} \mu_{20} & \mu_{11} \\ \mu_{11} & \mu_{02} \end{pmatrix}$$

$$M' = G^T M G = \begin{pmatrix} \lambda_1 & 0 \\ 0 & \lambda_2 \end{pmatrix} = \begin{pmatrix} \mu'_{20} & 0 \\ 0 & \mu'_{02} \end{pmatrix}$$

$$|M - \lambda I| = 0$$

$$\mu'_{20} \equiv \lambda_1 = [(\mu_{20}+\mu_{02})+\sqrt{(\mu_{20} - \mu_{02})^2 + 4\mu_{11}^2}]/2$$

$$\mu'_{02} \equiv \lambda_2 = [(\mu_{20}+\mu_{02})-\sqrt{(\mu_{20} - \mu_{02})^2 + 4\mu_{11}^2}]/2$$

# Reference ellipse

**An ellipse having the same 2nd order moments as the original object**

$$\mu'_{20} = \frac{\pi a^3 b}{4}$$

$$\mu'_{02} = \frac{\pi a b^3}{4}$$

*a, b* – major/minor semiaxis

## General construction of rotation invariants

**Complex moment**

$$c_{pq}^{(f)} = \int_{-\infty}^{\infty}\int_{-\infty}^{\infty}(x+iy)^p(x-iy)^q f(x,y)dxdy$$

Complex moment in polar coordinates

$$c_{pq}^{(f)} = \int_0^{\infty}\int_0^{2\pi} r^{p+q+1}e^{i(p-q)\theta} f(r,\theta)d\theta dr$$

## Basic relations between moments

$$c_{pq} = \sum_{k=0}^{p} \sum_{j=0}^{q} \binom{p}{k} \binom{q}{j} (-1)^{q-j} \cdot i^{p+q-k-j} \cdot m_{k+j,p+q-k-j}$$

$$m_{pq} = \frac{1}{2^{p+q} i^{q}} \sum_{k=0}^{p} \sum_{j=0}^{q} \binom{p}{k} \binom{q}{j} (-1)^{q-j} \cdot c_{k+j,p+q-k-j}$$

$$c_{qp} = c_{pq}^{*}$$

## Examples

$$c_{00} = m_{00}$$
$$c_{10} = m_{10} + i m_{01}$$
$$c_{20} = m_{20} - m_{02} + 2i m_{11}$$
$$c_{11} = m_{20} + m_{02}$$

$$m_{10} = (c_{10} + c_{01})/2$$
$$m_{20} = (c_{20} + 2c_{11} + c_{02})/4$$
$$m_{11} = (c_{20} - c_{02})/4i$$

## Rotation property of complex moments

$$f'(r,\theta) = f(r,\theta+\alpha)$$

$$c'_{pq} = e^{-i(p-q)\alpha} \cdot c_{pq}$$

The magnitude is preserved, the phase is shifted by $(p\text{-}q)\alpha$.

**Invariants are constructed by phase cancellation**

## Rotation invariants from complex moments

$$I = \prod_{i=1}^{n} c_{p_i q_i}^{k_i} \qquad \sum_{i=1}^{n} k_i(p_i - q_i) = 0$$

Examples:

$$c_{11}, c_{20}\cdot c_{02}, c_{20}\cdot c_{12}^2, \cdots, c_{pp}, c_{pq}\cdot c_{qp}, \cdots$$

**How to select a complete and independent subset (basis) of the rotation invariants?**

## Construction of the basis

$$\forall p, q : \qquad \Phi(p,q) \equiv c_{pq} c_{q_0 p_0}^{p-q}$$

$$\begin{aligned} & p + q \leq r \\ & p \geq q \\ & p_0 + q_0 \leq r \\ & p_0 - q_0 = 1 \\ & c_{p_0 q_0} \neq 0 \end{aligned}$$

This is the basis of invariants up to the order *r*

## Inverse problem

$$\begin{aligned} \Phi(p_0, q_0) &= c_{p_0 q_0} c_{q_0 p_0} \\ \Phi(0,0) &= c_{00} \\ \Phi(1,0) &= c_{10} c_{q_0 p_0} \\ \Phi(2,0) &= c_{20} c_{q_0 p_0}^2 \\ \Phi(1,1) &= c_{11} \\ \Phi(3,0) &= c_{30} c_{q_0 p_0}^3 \\ &\cdots \\ \Phi(r,0) &= c_{r0} c_{q_0 p_0}^r \\ \Phi(r-1,1) &= c_{r-1,1} c_{q_0 p_0}^{r-2} \\ &\cdots \end{aligned}$$

Is it possible to resolve this system ?

## Inverse problem - solution

Normalization constraint:
$c_{p_0 q_0}$ real and positive

$$c_{p_0 q_0} = \sqrt{\Phi(p_0, q_0)}$$
$$c_{pq} = \frac{\Phi(p, q)}{c_{q_0 p_0}^{p-q}}$$

## The basis of the 3rd order

$p_0 = 2,\ q_0 = 1$

$$\begin{aligned}
\Phi(1,1) &= c_{11} \\
\Phi(2,1) &= c_{21} c_{12} \\
\Phi(2,0) &= c_{20} c_{12}^2 \\
\Phi(3,0) &= c_{30} c_{12}^3
\end{aligned}$$

This is basis $B_3$ (contains six real elements)

## Comparing $B_3$ to the Hu's set

$$\begin{aligned}
\phi_1 &= c_{11} \\
\phi_2 &= c_{20}c_{02} \\
\phi_3 &= c_{30}c_{03} \\
\phi_4 &= c_{21}c_{12} \\
\phi_5 &= \mathrm{Re}(c_{30}c_{12}^3) \\
\phi_6 &= \mathrm{Re}(c_{20}c_{12}^2) \\
\phi_7 &= \mathrm{Im}(c_{30}c_{12}^3)
\end{aligned}$$

$$\begin{aligned}
\phi_1 &= \Phi(1,1) \\
\phi_2 &= \frac{|\Phi(2,0)|^2}{\Phi(2,1)^2} \\
\phi_3 &= \frac{|\Phi(3,0)|^2}{\Phi(2,1)^3} \\
\phi_4 &= \Phi(2,1) \\
\phi_5 &= \mathrm{Re}(\Phi(3,0)) \\
\phi_6 &= \mathrm{Re}(\Phi(2,0)) \\
\phi_7 &= \mathrm{Im}(\Phi(3,0))
\end{aligned}$$

## Normalized position to rotation by means of complex moments

$$c_{st} \text{ real and positive} \Longrightarrow$$

$$\alpha = \frac{1}{s-t} \cdot \arctan\left(\frac{\mathrm{Im}c_{st}}{\mathrm{Re}c_{st}}\right)$$

## Invariants to contrast changes

$$f'(x,y) = c \cdot f(x,y)$$

$$\mu'_{pq} = c \cdot \mu_{pq}$$

$$C_{pq} = \frac{\mu_{pq}}{\mu_{00}}$$

## Invariants to contrast and scaling

$$\frac{\mu_{pq}}{\mu_{00}^{1-\beta} \cdot \mu_{20}^{\beta}}, \qquad \beta = \frac{p+q}{2}$$

# Invariants to convolution

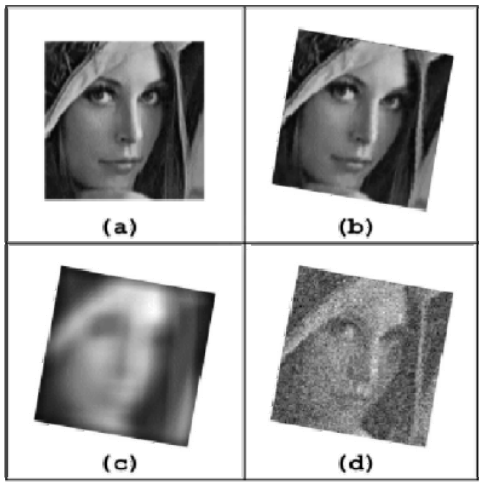


**I(f) = I(f*h)  for any admissible h**

$$g(x, y) = (f * h)(x, y) + n(x, y)$$

## Two approaches

**Traditional approach: Image restoration (blind deconvolution)**

**Proposed approach:  Invariants to convolution**

# The moments under convolution

$$c_{pq}^{(f)} = \int_{-\infty}^{\infty}\int_{-\infty}^{\infty}(x+iy)^p(x-iy)^q f(x,y)dxdy$$

*f(x,y)* … image function

*h(x,y)* … shift invariant PSF of a linear imaging system

*g(x,y)* … blurred image $g(x,y) = (f * h)(x,y)$

$$c_{pq}^{(g)} = \sum_{k=0}^{p}\sum_{j=0}^{q}\binom{p}{k}\binom{q}{j}c_{kj}^{(h)}c_{p-k,q-j}^{(f)}$$

# Assumptions on the PSF

## Our assumption: PSF is centrosymmetric

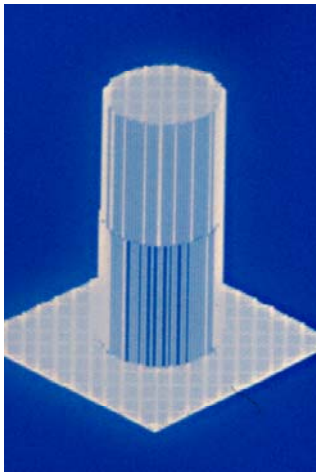

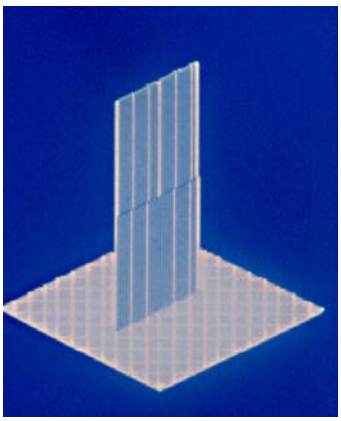

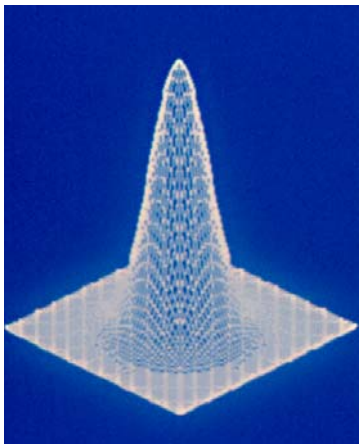

# Invariants to convolution

- PSF is centrosymmetric

$$K(p,q)^{(f)} = c_{pq}^{(f)} - \frac{1}{c_{00}^{(f)}} \sum_{n=0}^{p} \sum_{\substack{m=0 \\ 0<n+m<p+q}}^{q} \binom{p}{n}\binom{q}{m} K(p-n,q-m)^{(f)} \cdot c_{nm}^{(f)}$$

where ($p$ + $q$) is odd

# Other assumptions on the PSF

The more we know about the PSF, the more invariants and the higher discriminability we get.

If PSF is circularly symmetric, then we have invariants of the form

$$R(p,q)^{(f)} = c_{pq}^{(f)} - \frac{1}{c_{00}^{(f)}} \sum_{n=1}^{q} \binom{p}{n}\binom{q}{n} R(p-n,q-n)^{(f)} \cdot c_{nn}^{(f)}$$

where $p > q$.

## Discrimination power

- The null-space of the blur invariants
- Intuitive meaning of the invariants
- The number of the invariants

# Combined moment invariants

$$K'(p,q) = e^{-i(p-q)\alpha} \cdot K(p,q)$$

$$I = \prod_{j=1}^{n} K(p_j, q_j)^{k_j} \quad ; \quad \sum_{j=1}^{n} k_j (p_j - q_j) = 0$$

## Invariants to convolution and rotation

***I(f) = I(R(f*h))*** **for any admissible *h* and rotation *R***

# Robustness of the invariants

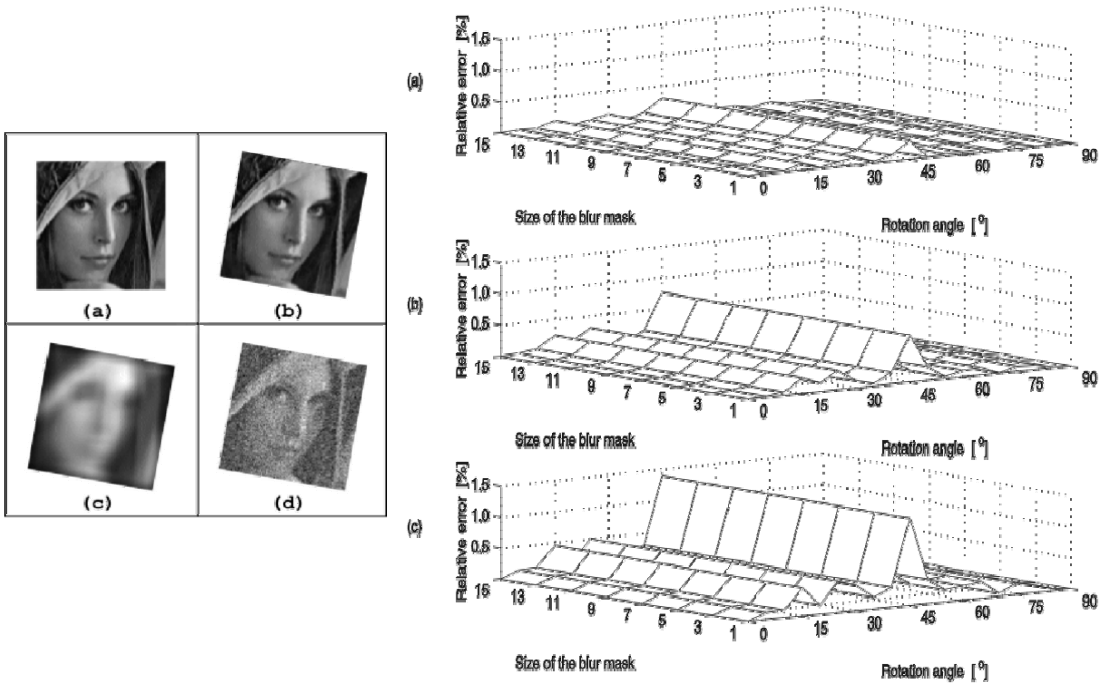


# Convolution invariants in FT domain

$$
\begin{aligned}
g &= f * h \\
G &= F \cdot H \\
|G| &= |F| \cdot |H| \\
\mathrm{ph}G &= \mathrm{ph}F + \mathrm{ph}H
\end{aligned}
$$

## Convolution invariants in FT domain

$$\text{Centrosymmetric } h(x,y) \Longrightarrow \text{real } H(u,v)$$

$$\text{ph}H \in \{0;\pi\}$$

$$\tan(\text{ph}G) = \tan(\text{ph}F)$$

## Relationship between FT and moment invariants

$$\tan(\text{ph}F(u,v)) = \frac{1}{\mu_{00}} \sum_{p=0}^{\infty} \sum_{q=0}^{\infty} C(p,q) \cdot u^p v^q \frac{(-1)^{(p+q-1)/2} \cdot (-2\pi)^{(p+q)}}{p! \cdot q!}$$

# Moment-based focus measure

- Odd-order moments → blur invariants
- Even-order moments → blur/focus measure

$$M(g) = \mu_{20}^{(g)} + \mu_{02}^{(g)} = (\mu_{20}^{(f)} + \mu_{02}^{(f)}) + \mu_{00}^{(f)} (\mu_{20}^{(h)} + \mu_{02}^{(h)})$$

If $M(g1) > M(g2)$ → $g2$ is less blurred (more focused)

## Desirable properties of a focus measure

- Agreement with a visual assessment
- Unimodality
- Robustness to noise
- Robustness to small image changes
- Robustness to restoration artefacts

Moments are generally worse than wavelets and other differential focus measures because they are too sensitive to local changes but they are very robust to noise.

## Rotation invariants for recognition of symmetric objects

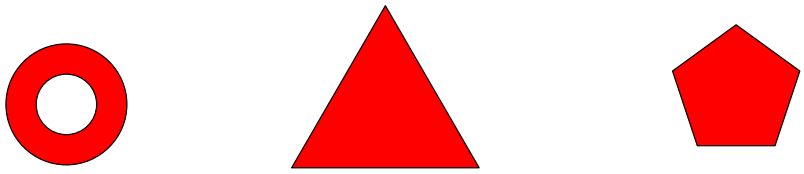

$N$-fold rotation symmetry: the object repeats itself when rotating by $2\pi j/N$ for all $j = 1, \cdots, N$.

## Difficulties with symmetric objects

Many moments and many invariants are zero

If $f(x,y)$ has $N$–fold rotation symmetry then

$$c_{pq} = 0$$

for every $p, q$ such that $(p-q)/N$ is not an integer.

## Difficulties with symmetric objects

The greater *N*, the less nontrivial invariants

Particularly

- $N = 1$ (no symmetry) $\Longrightarrow$ previous case
- $N = 2$ (central symmetry) $\Longrightarrow$ only even-order invariants exist
- $N = \infty$ (circular symmetry) $\Longrightarrow$ only $\Phi(p,p) \equiv c_{pp}$

## Difficulties with symmetric objects

**It is very important to use only non-trivial invariants**

**The choice of appropriate invariants (basis of invariants) depends on *N***

## The basis for *N*-fold symmetric objects

Generalization of the previous theorem

$$\forall p, q: \qquad \Phi(p,q) \equiv c_{pq} c^{k}_{q_0 p_0}$$

$$\begin{aligned}
&k = (p-q)/N \\
&p + q \leq r \\
&p \geq q \\
&p_0 + q_0 \leq r \\
&p_0 - q_0 = N \\
&c_{p_0 q_0} \neq 0
\end{aligned}$$

$\langle \mathcal{B} \rangle$ – all rotation invariants generated from $\mathcal{B}$

- $M, N$ finite, $L$ – least common multiple

$$\langle \mathcal{B}_M \rangle \cap \langle \mathcal{B}_N \rangle = \langle \mathcal{B}_L \rangle$$

If $M/N$ is integer then $\langle \mathcal{B}_M \rangle \subset \langle \mathcal{B}_N \rangle$

- $$\bigcap_{N=1}^{\infty} \langle \mathcal{B}_N \rangle = \langle \mathcal{B}_\infty \rangle$$

- $$|\mathcal{B}_N| = \sum_{j=0}^{n} [\frac{r - jN + 2}{2}]$$

where $n = [r/N]$

$$|\mathcal{B}_\infty| = [\frac{r+2}{2}]$$

## Recognition of symmetric objects – Experiment 1

**5 objects with *N* = 3**

## Recognition of symmetric objects – Experiment 1

Bad choice: $p_0 = 2$, $q_0 = 1$

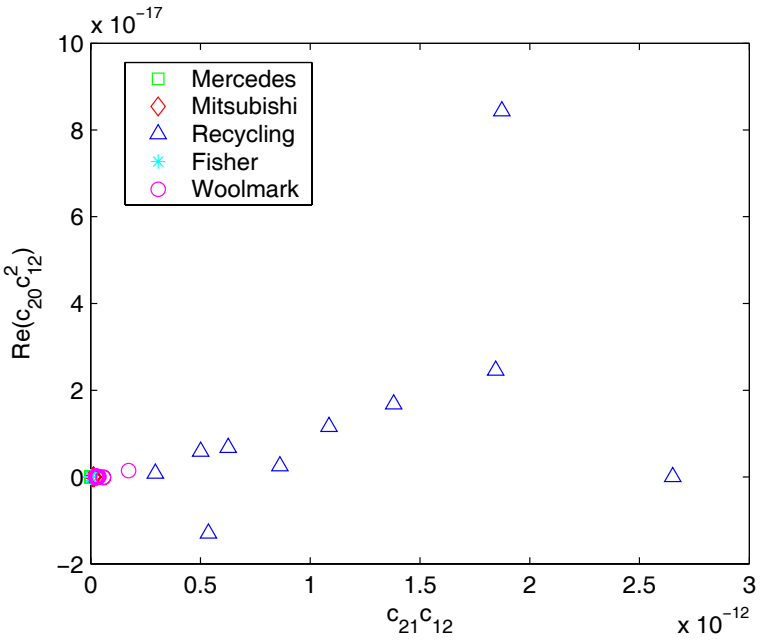


## Recognition of symmetric objects – Experiment 1

Optimal choice: $p_0 = 3$, $q_0 = 0$

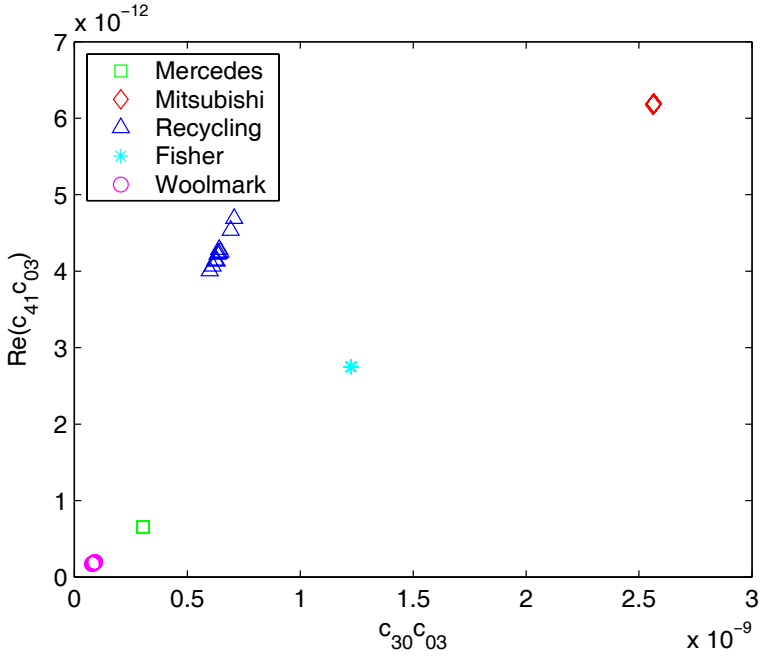

## Recognition of symmetric objects – Experiment 2

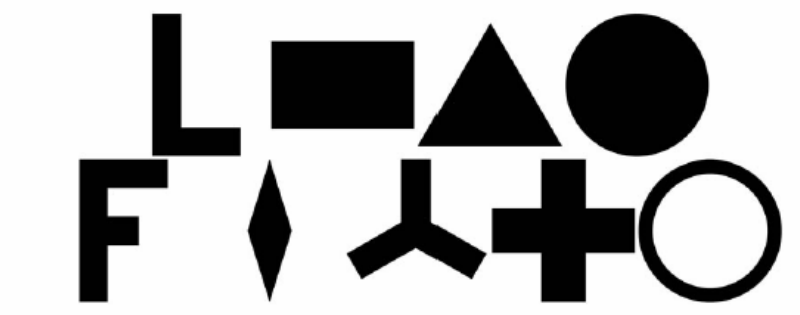

**2 objects with $N = 1$**

**2 objects with $N = 2$**

**2 objects with $N = 3$**

**1 object with $N = 4$**

**2 objects with $N = \infty$**

## Recognition of symmetric objects – Experiment 2

Bad choice: $p_0 = 2$, $q_0 = 1$

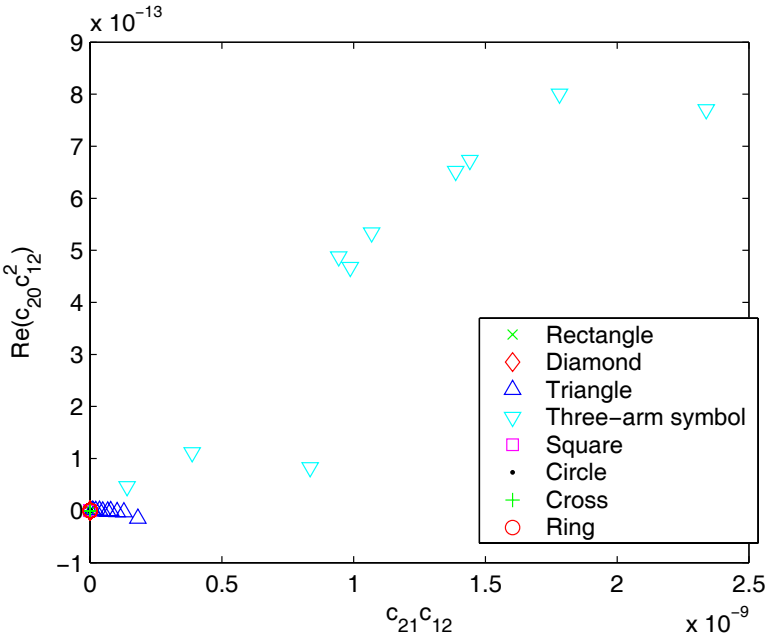

## Recognition of symmetric objects – Experiment 2

Better choice: $p_0 = 4$, $q_0 = 0$

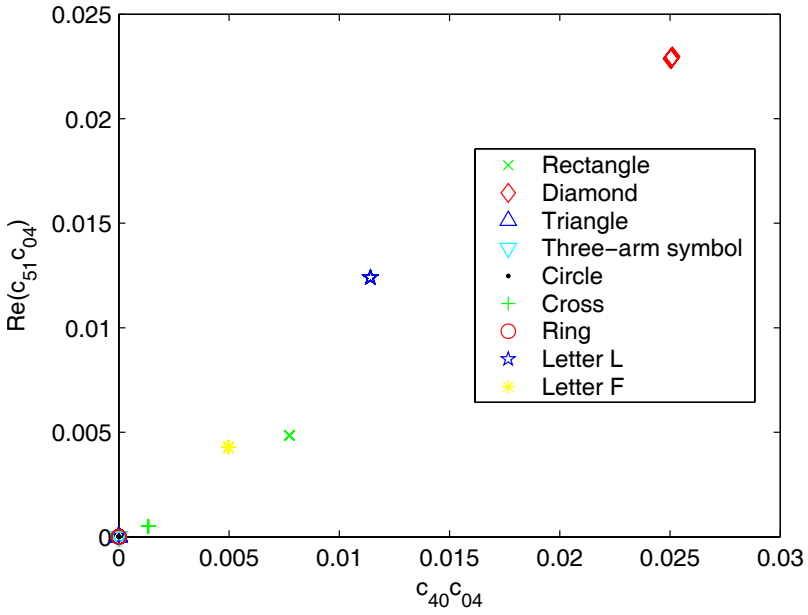


## Recognition of symmetric objects – Experiment 2

Theoretically optimal choice: $p_0 = 12$, $q_0 = 0$

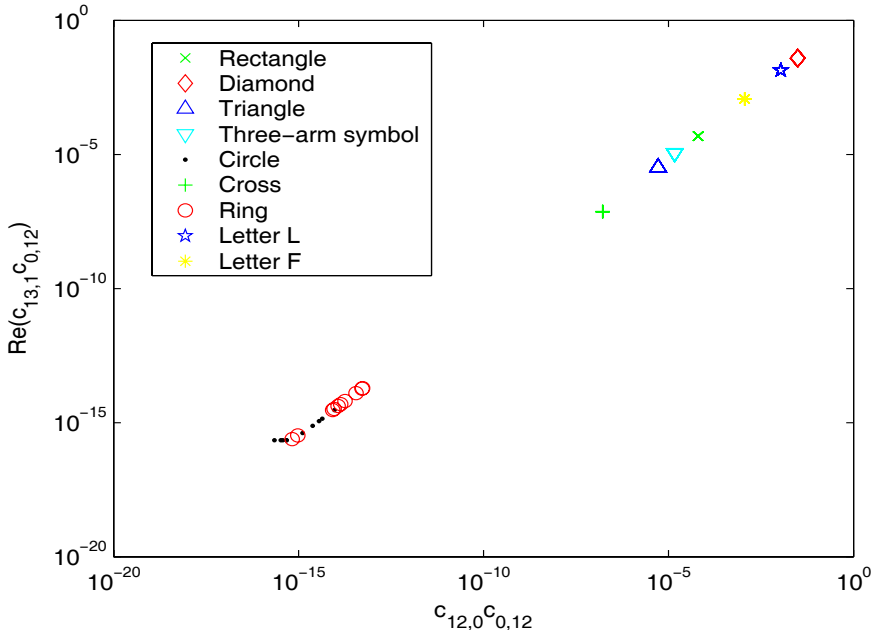


Logarithmic scale

## Recognition of symmetric objects – Experiment 2

The best choice: mixed orders

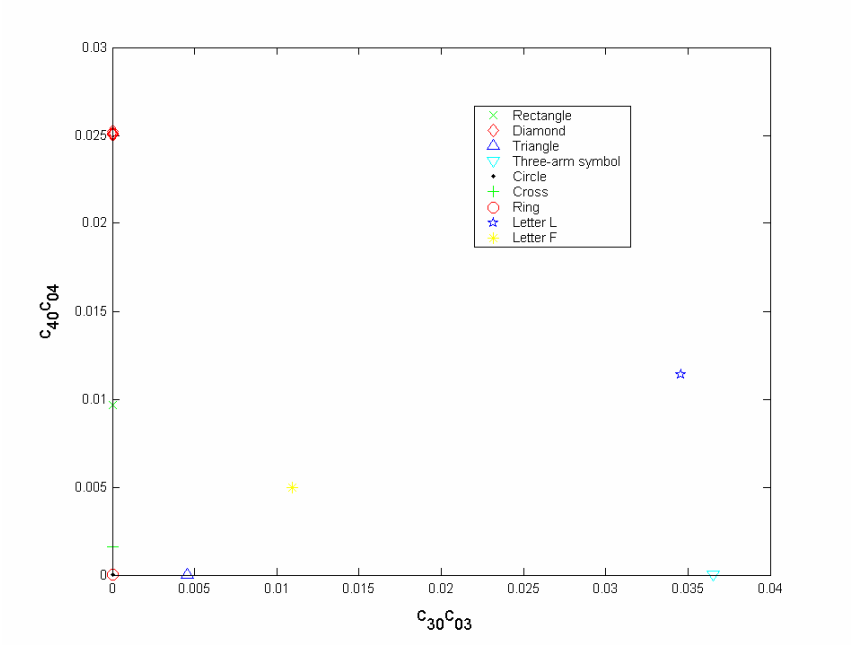


# Invariants to affine transform

## What is affine transform?

$$u = a_1 x + a_2 y + a_0$$
$$v = b_1 x + b_2 y + b_0$$

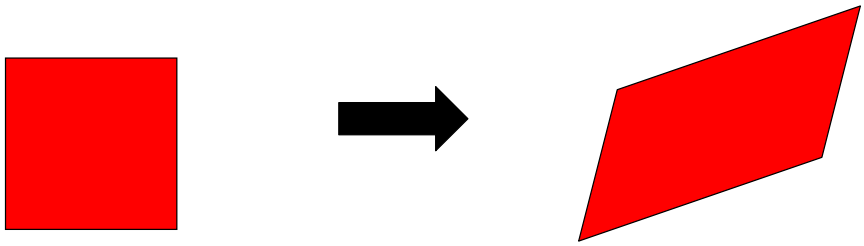

## Why is affine transform important?

- Affine transform is a good approximation of projective transform
- Projective transform describes a perspective projection of 3-D objects onto 2-D plane by a central camera

$$u = \frac{a_0 + a_1 x + a_2 y}{1 + c_1 x + c_2 y}$$

$$v = \frac{b_0 + b_1 x + b_2 y}{1 + c_1 x + c_2 y}$$

## Affine moment invariants

**Many ways how to derive them**

- Theory of algebraic invariants (Hilbert, Schur, Gurewich)
- Tensor algebra, Group theory (Lenz, Meer)
- Algebraic invariants revised (Reiss, Flusser & Suk, Mamistvalov)
- Image normalization (Rothe et al.)
- Graph theory (Flusser & Suk)
- Hybrid approaches

**All methods lead to the same invariants**

$$I_1 = (\mu_{20}\mu_{02} - \mu_{11}^2)/\mu_{00}^4$$

$$I_2 = (\mu_{30}^2\mu_{03}^2 - 6\mu_{30}\mu_{21}\mu_{12}\mu_{03} + 4\mu_{30}\mu_{12}^3 + 4\mu_{03}\mu_{21}^3 - 3\mu_{21}^2\mu_{12}^2)/\mu_{00}^{10}$$

$$I_3 = (\mu_{20}(\mu_{21}\mu_{03} - \mu_{12}^2) - \mu_{11}(\mu_{30}\mu_{03} - \mu_{21}\mu_{12}) + \mu_{02}(\mu_{30}\mu_{12} - \mu_{21}^2))/\mu_{00}^7$$

## General construction of Affine Moment Invariants

$(x_1, y_1), (x_2, y_2)$ – arbitrary points

$$C_{12} = x_1 y_2 - x_2 y_1$$

$$C'_{12} = J \cdot C_{12}$$

$N$ points, $n_{kj}$ – non-negative integers

$$I(f) = \int_{-\infty}^{\infty} \prod_{k,j=1}^{N} C_{kj}^{n_{kj}} \cdot \prod_{i=1}^{N} f(x_i, y_i) dx_i dy_i$$

## General construction of Affine Moment Invariants

$$I' = J^w |J|^N \cdot I$$

where

$$w = \sum_{k,j} n_{kj}$$

### Affine Moment Invariants

$$\left(\frac{I}{\mu_{00}^{w+N}}\right)' = \left(\frac{I}{\mu_{00}^{w+N}}\right)$$

## Simple examples of the AMI's

2) $N = 3,\ n_{12} = 2,\ n_{13} = 2,\ n_{23} = 0$

$$I(f) = \int_{-\infty}^{\infty} (x_1 y_2 - x_2 y_1)^2 (x_1 y_3 - x_3 y_1)^2$$

$$f(x_1, y_1) f(x_2, y_2) f(x_3, y_3) dx_i dy_i$$

$$= m_{20}^2 m_{04} - 4 m_{20} m_{11} m_{13} + 2 m_{20} m_{02} m_{22} +$$

$$4 m_{11}^2 m_{22} - 4 m_{11} m_{02} m_{31} + m_{02}^2 m_{40}$$

## Graph representation of the AMI's

$(x_k, y_k)$ – a node of the graph

$C_{kj}$ – an edge of the graph

$C_{kj}^{n_{kj}}$ – $n_{kj}$ edges

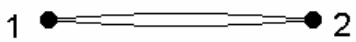


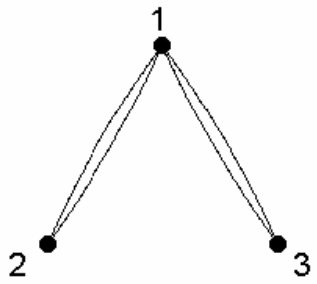


## Graph representation of the AMI's

$$I_2 = (-\mu_{30}^2\mu_{03}^2 + 6\mu_{30}\mu_{21}\mu_{12}\mu_{03} - 4\mu_{30}\mu_{12}^3 - 4\mu_{21}^3\mu_{03} + 3\mu_{21}^2\mu_{12}^2)/\mu_{00}^{10}$$

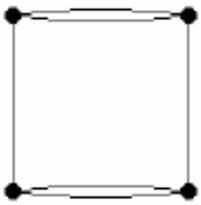

## Graph representation of the AMI's

$$I_3 = (\mu_{20}\mu_{21}\mu_{03} - \mu_{20}\mu_{12}^2 - \mu_{11}\mu_{30}\mu_{03} + \mu_{11}\mu_{21}\mu_{12} + \mu_{02}\mu_{30}\mu_{12} - \mu_{02}\mu_{21}^2)/\mu_{00}^7$$

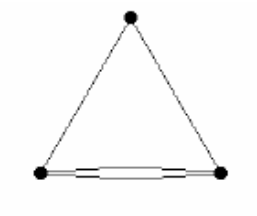

## Graph representation of the AMI's

$$I_7 = (\mu_{40}\mu_{22}\mu_{04} - \mu_{40}\mu_{13}^2 - \mu_{31}^2\mu_{04} + 2\mu_{31}\mu_{22}\mu_{13} - \mu_{22}^3)/\mu_{00}^9$$

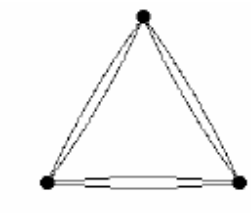

## Graph representation of the AMI's

$$
\begin{aligned}
I_{352} \;=\; & (\mu_{20}^5\mu_{0,10} - 10\mu_{20}^4\mu_{11}\mu_{19} + 5\mu_{20}^4\mu_{02}\mu_{28} + 40\mu_{20}^3\mu_{11}^2\mu_{28} - 40\mu_{20}^3\mu_{11}\mu_{02}\mu_{37} \\
& +10\mu_{20}^3\mu_{02}^2\mu_{46} - 80\mu_{20}^2\mu_{11}^3\mu_{37} + 120\mu_{20}^2\mu_{11}^2\mu_{02}\mu_{46} - 60\mu_{20}^2\mu_{11}\mu_{02}^2\mu_{55} \\
& +10\mu_{20}^2\mu_{02}^3\mu_{64} + 80\mu_{20}\mu_{11}^4\mu_{46} - 160\mu_{20}\mu_{11}^3\mu_{02}\mu_{55} + 120\mu_{20}\mu_{11}^2\mu_{02}^2\mu_{64} \\
& -40\mu_{20}\mu_{11}\mu_{02}^3\mu_{73} + 5\mu_{20}\mu_{02}^4\mu_{82} - 32\mu_{11}^5\mu_{55} + 80\mu_{11}^4\mu_{02}\mu_{64} - 80\mu_{11}^3\mu_{02}^2\mu_{73} \\
& +40\mu_{11}^2\mu_{02}^3\mu_{82} - 10\mu_{11}\mu_{02}^4\mu_{91} + \mu_{02}^5\mu_{10,0})/\mu_{00}^{16}
\end{aligned}
$$

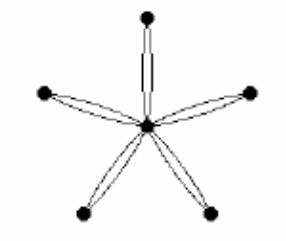

## Affine invariants via normalization

**Many possibilities how to define normalization constraints**

**Several possible decompositions of affine transform**

## Decomposition of the affine transform

- Horizontal and vertical translation
- Scaling
- First rotation
- Stretching
- Second rotation
- Mirror reflection

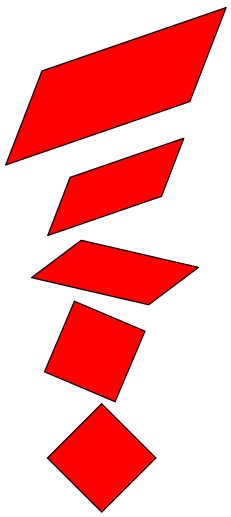

## Normalization to partial transforms

- Horizontal and vertical translation -- $m_{01} = m_{10} = 0$
- Scaling -- $c_{00} = 1$
- First rotation -- $c_{20}$ real and positive
- Stretching -- $c_{20} = 0$ $(\mu_{20} = \mu_{02})$
- Second rotation -- $c_{21}$ real and positive

## Properties of the AMI's

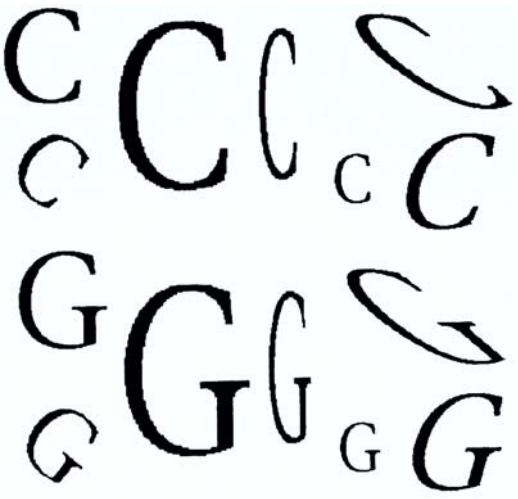

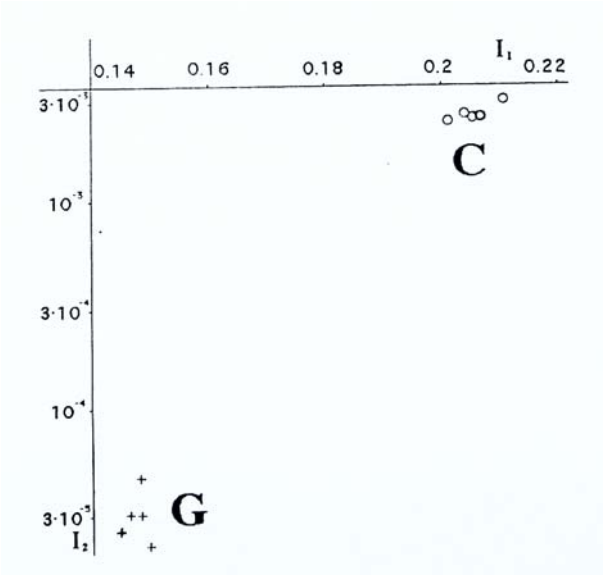


## Application of the AMI's

- Recognition of distorted shapes
- Image registration

# Clusters in the space of the AMI's

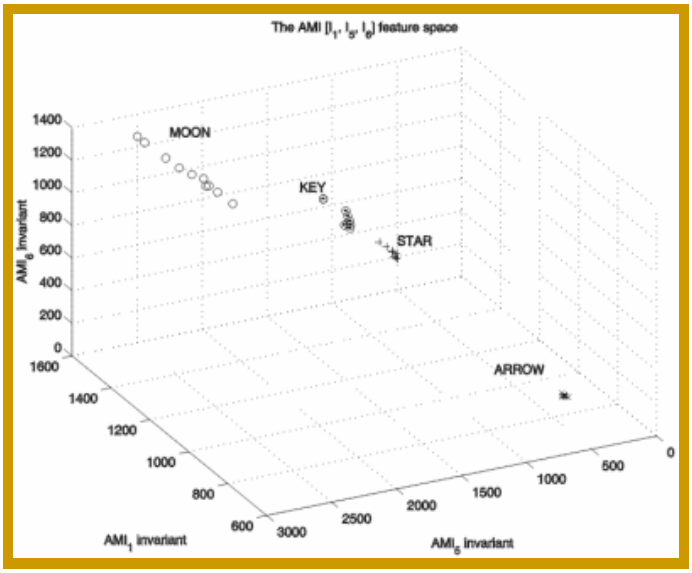


# Aspect-ratio invariants

$$u = a \cdot x$$
$$v = b \cdot y$$

$$\mu'_{pq} = a^{p+1} b^{q+1} \mu_{pq}$$

$$A_{pq} = \frac{\mu_{00}^{(p+q+2)/2}}{\mu_{20}^{(p+1)/2} \cdot \mu_{02}^{(q+1)/2}} \cdot \mu_{pq}$$

## Projective moment invariants

Projective transform describes a perspective projection of 3-D objects onto 2-D plane by a central camera

$$u = \frac{a_0 + a_1 x + a_2 y}{1 + c_1 x + c_2 y}$$

$$v = \frac{b_0 + b_1 x + b_2 y}{1 + c_1 x + c_2 y}$$

## Projective moment invariants

- Do not exist using any finite set of moments
- Do not exist using infinite set of (all) moments
- Exist formally as infinite series of moments of both positive and **negative** indexes

## Combined blur-affine invariants

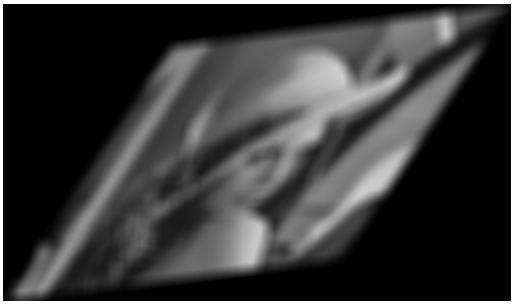

- Let *I(μ00,…, μPQ)* be an affine moment invariant. Then *I(C(0,0),…,C(P,Q))*, where *C(p,q)* are blur invariants, is a combined blur-affine invariant.

## Examples

$$I_1 = (\mu_{30}^2\mu_{03}^2 - 6\mu_{30}\mu_{21}\mu_{12}\mu_{03} + 4\mu_{30}\mu_{12}^3 + 4\mu_{21}^3\mu_{03} - 3\mu_{21}^2\mu_{12}^2)/\mu_{00}^{10}$$

$$\begin{aligned} I_2 = (&\mu_{50}^2\mu_{05}^2 - 10\mu_{50}\mu_{41}\mu_{14}\mu_{05} + 4\mu_{50}\mu_{32}\mu_{23}\mu_{05} + 16\mu_{50}\mu_{32}\mu_{14}^2 \\ &- 12\mu_{50}\mu_{23}^2\mu_{14} + 16\mu_{41}^2\mu_{23}\mu_{05} + 9\mu_{41}^2\mu_{14}^2 - 12\mu_{41}\mu_{32}^2\mu_{05} \\ &- 76\mu_{41}\mu_{32}\mu_{23}\mu_{14} + 48\mu_{41}\mu_{23}^3 + 48\mu_{32}^3\mu_{14} - 32\mu_{32}^2\mu_{23}^2)/\mu_{00}^{14} \end{aligned}$$

$$C(3,0) = \mu_{30}$$
$$C(2,1) = \mu_{21}$$

$$C(5,0) = \mu_{50} - 10\mu_{30}\mu_{20}/\mu_{00}$$
$$C(4,1) = \mu_{41} - 2(3\mu_{21}\mu_{20} + 2\mu_{30}\mu_{11})/\mu_{00}$$
$$C(3,2) = \mu_{32} - (3\mu_{12}\mu_{20} + \mu_{30}\mu_{02} + 6\mu_{21}\mu_{11})/\mu_{00}$$

## Orthogonal moments

$$\{\mathcal{P}_{pq}(x,y)\} - \text{set of orthogonal polynomials}$$

$$M_{pq} = \int\int \mathcal{P}_{pq}(x,y) f(x,y) dx dy$$

- Legendre
- Zernike
- Fourier-Mellin
- Czebyshev
- Krawtchuk, Hahn

## Two reasons for using OG moments

- Avoiding numerical problems with high values, recurrent calculations
- Image reconstruction

$$f(x,y) = \sum_p \sum_q M_{pq} \mathcal{P}_{pq}(x,y)$$

# Image reconstruction from geometric moments

$$F(u,v) = \sum_p \sum_q \frac{(-2\pi i)^{p+q}}{p!q!} m_{pq} u^p v^q$$

# Standard powers

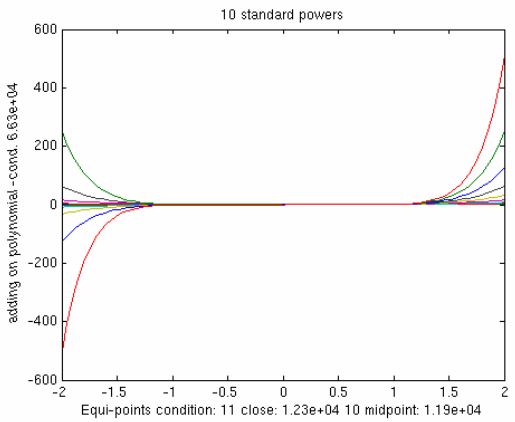


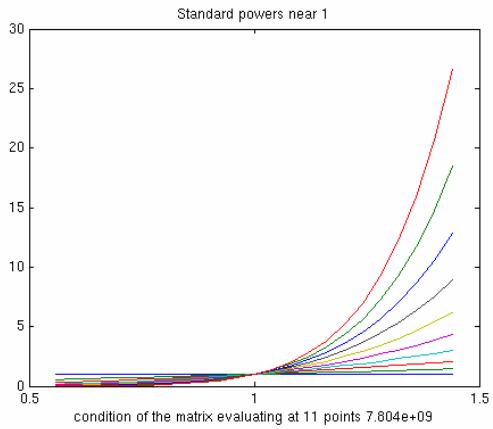

# OG Czebyshev polynomials

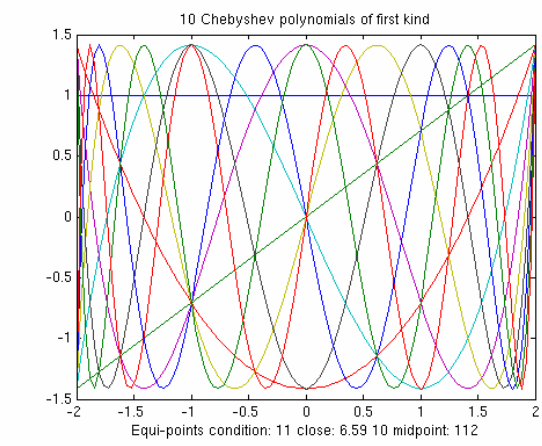


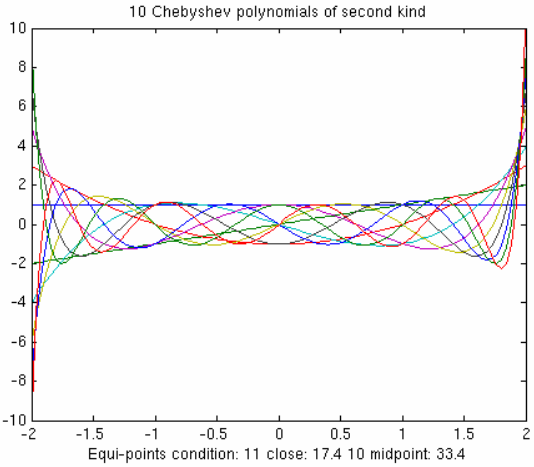


# Legendre polynomials

## Definition

$$P_n(x) = \frac{1}{2^n n!}\frac{\partial^n}{\partial x^n}(x^2-1)^n$$

## Orthogonality

$$\int_{-1}^{1} P_n(x)P_m(x)dx = \frac{2}{2m+1}\delta_{mn}$$

## Legendre polynomials

$$P_0(x) = 1$$

$$P_1(x) = x$$

$$P_2(x) = \frac{3x^2-1}{2}$$

$$P_3(x) = \frac{5x^3-3x}{2}$$

## Legendre moments

$$L_{pq} = \frac{(2p+1)(2q+1)}{4} \int_{-1}^{1} \int_{-1}^{1} P_p(x) P_q(y) f(x,y) dx dy$$

$$L_{pq} = \frac{(2p+1)(2q+1)}{4} \sum_{k=0}^{p} \sum_{j=0}^{q} a_{pk} a_{qj} m_{kj}$$

## Legendre moments

$$L_{00} = m_{00}$$

$$L_{10} = \frac{3}{4} m_{00}$$

$$L_{20} = \frac{5}{8}(3m_{20} - m_{00})$$

$$L_{11} = \frac{9}{4} m_{11}$$

## Zernike polynomials

Definition

$$V_{nm}(r,\theta) = R_{nm}(r) e^{im\theta}$$

$$R_{nm}(r) = \sum_{k=m}^{n} b_k r^k$$

Orthogonality

$$\int_0^{2\pi} \int_0^1 V_{nj}^*(r,\theta) V_{mk}(r,\theta) r dr d\theta = \frac{\pi}{n+1} \delta_{mn} \delta_{jk}$$

## Zernike moments

$$Z_{pq} = \frac{p+1}{\pi} \int_0^{2\pi} \int_0^1 V_{pq}^*(r,\theta) f(r,\theta) r dr d\theta$$

$$= \frac{p+1}{\pi} \sum_{k=q}^{p} b_k c_{(k-q)/2,(k+q)/2}$$

## Zernike moments

$$Z_{00} = \frac{1}{\pi} m_{00}$$

$$Z_{11} = \frac{2}{\pi}(m_{10} - i m_{01})$$

$$Z_{20} = \frac{6}{\pi}(m_{20} + m_{02}) - \frac{3}{\pi} m_{00}$$

## Rotation property of Zernike moments

$$Z'_{pq} = e^{-iq\alpha} \cdot Z_{pq}$$

The magnitude is preserved, the phase is shifted by $q\alpha$.

**Invariants are constructed by phase cancellation**

## Rotation invariants from Zernike moments

$$I = \prod_{j=1}^{n} Z_{p_j q_j}^{k_j} \qquad \sum_{j=1}^{n} k_j q_j = 0$$

# Moments in a discrete domain

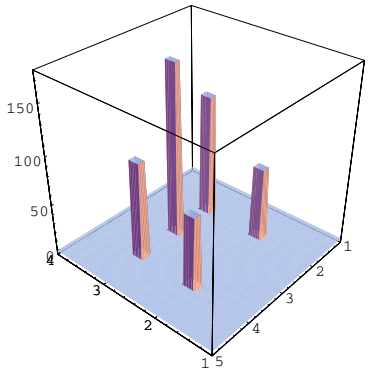


$$m_{pq}^{(f)} = \sum_{j,k=-\infty}^{+\infty} j^p k^q f_{jk}$$

# Fast moment calculation for binary objects

$$m_{pq}^{G} = \sum_{i=1}^{N} \sum_{j=1}^{N} i^p j^q f_{ij} = \sum_{(i,j)\in G} i^p j^q$$

- Decomposition methods
- Boundary-based methods

## Decomposition methods

- Rows (Delta method)
- Row segments (Philips)
- Blocks of rows
- Bin-tree, quad-tree

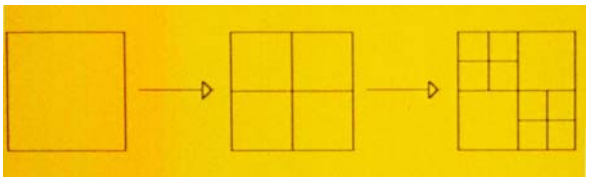

- Morphologic decomposition

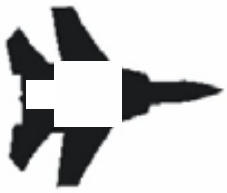

## Boundary-based methods

Green's theorem

$$\int\int_G \frac{\partial}{\partial x} g(x,y)dxdy = \oint_{\partial G} g(x,y)dy$$

$$g(x,y) = \frac{x^{p+1}y^q}{p+1}$$

$$m_{pq}^G = \frac{1}{p+1}\oint_{\partial G} x^{p+1}y^q dy$$

## Calculation of the boundary integral

- Summation pixel-by-pixel
- Polygonal approximation
- Other approximations (splines, etc.)

## Summary: Are moments good features for object recognition?

- **YES, because of**
  - **well-developed mathematics behind, invariance to many transformations**
  - **complete and independent set**
  - **good discrimination power**
  - **robust to noise**
- **NO, because**
  - **moments are global**
  - **small local disturbance affects all moments**
  - **careful object segmentation is required**

More about this tutorial on

http://staff.utia.cas.cz/zitova/tutorial/

# Abstract

This tutorial aims to present a survey of recent as well as traditional object recognition/classification methods based on image moments. We review various types of moments (geometric moments, complex moments, Legendre moments, Zernike and Pseudo-Zernike moments, and Fourier-Mellin moments) and moment-based invariants with respect to various image degradations and distortions (rotation, scaling, affine transform, image blurring, etc.) which can be used as shape features for classification. We explain a general theory how to construct these invariants and show also a few of them in explicit forms. We review efficient numerical algorithms that can be used for moment computation. Finally, we demonstrate practical examples of using moment invariants in real applications from the area of vision, remote sensing, and medical imaging.

The target audience of the tutorial are

- researchers from all application areas who need to recognize 2-D objects extracted from binary/graylevel/color images and who look for invariant and robust object features,
- specialists in moment-based pattern recognition interested in new development on this field.

**Keywords:** Object recognition, degraded images, moments, moment invariants, geometric invariants, invariants to convolution, moment computation.

# 1 Introduction

Analysis and interpretation of an image which was acquired by a real (i.e. non-ideal) imaging system is the key problem in many application areas such as remote sensing, astronomy and medicine, among others. Since real imaging systems as well as imaging conditions are usually imperfect, the observed image represents only a degraded version of the original scene. Various kinds of degradations (geometric as well as radiometric) are introduced into the image during the acquisition by such factors as imaging geometry, lens aberration, wrong focus, motion of the scene, systematic and random sensor errors, etc. (see Figs. 1, 2, and 3 for illustrative examples).

Figure 1: Image blurring caused by wrong focus of the camera.

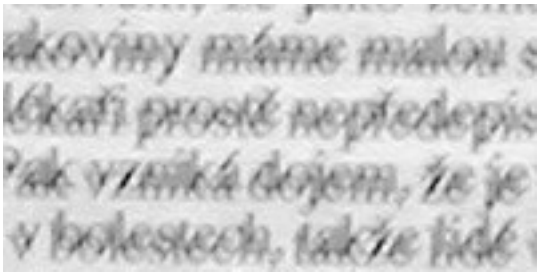

Figure 2: Image blurring caused by random vibrations of the object.

In the general case, the relation between the ideal image $f(x, y)$ and the observed image $g(x, y)$ is described as $g = \mathcal{D}(f)$, where $\mathcal{D}$ is a degradation operator. In the case of a linear shift-invariant imaging system, $\mathcal{D}$ has a form of

$$g(\tau(x, y)) = (f * h)(x, y) + n(x, y), \tag{1}$$

where $h(x, y)$ is the point-spread function (PSF) of the system, $n(x, y)$ is an additive random noise, $\tau$ is a transform of spatial coordinates due to projective imaging geometry

Figure 3: Image distortion caused by a non-standard lens along with motion blur.

and $*$ denotes a 2-D convolution. Knowing the image $g(x, y)$, our objective is to analyze the unknown scene $f(x, y)$.

By the term "scene analysis" we usually understand a complex process consisting of three basic stages. First, the image is segmented in order to extract objects of potential interest. Secondly, the extracted objects are "recognized", which means they are classified as elements of one class from the set of pre-defined object classes. Finally, spatial relations among the objects can be analyzed. In this tutorial, we focus on object recognition.

Recognition of objects and patterns that are deformed in various ways has been a goal of much recent research. There are basically three major approaches to this problem – brute force, image normalization, or invariant features. In brute force approach we search the space of all possible image degradations. That means the training set of each class should consist not only all class representatives but also all their rotated, scaled, blurred, and deformed versions. Clearly, this approach would lead to extreme time complexity and is practically inapplicable. In normalization approach, the objects are transformed into some standard position before they are classified. This could be very efficient in the classification stage but the object normalization usually requires to solve complex inverse problems which are often ill posed. The approach using invariant features appears to be the most promising. Its basic idea is to describe the objects by a set of features which are not sensitive to particular deformations and which provide enough discrimination power to distinguish among objects from different classes. From mathematical point of view, we have to find functional $I$ defined on the space of all admissible image functions (let's imagine $L_1(R^2)$ space for instance) which are invariant with respect to degradation operator $\mathcal{D}$, i.e. which satisfies the condition $I(f) = I(\mathcal{D}(f))$ for any image function $f$.

In this tutorial we present non-linear invariant functionals, which are composed of various projections of $f$ into the space of polynomials. Such projections are known as *image moments* and the respective functionals are called *moment invariants*. We present several groups of moment invariants with respect to the most common degradations –

image rotation and scaling, image affine transform, and image blurring (convolution with an unknown filter). We explain a general theory how to construct these functionals and show also a few of them in explicit forms. Then we discuss numerical algorithms for efficient moment calculation. In the last section, practical examples of using moment invariants in real applications from the area of computer vision, remote sensing, and medical imaging are demonstrated.

# 2 History

The history of moment invariants begun many years before the appearance of first computers, in the 19th century under the framework of the theory of algebraic invariants. The theory of algebraic invariants probably originate from famous German mathematician David Hilbert [1][1] and was thoroughly studied also in [2], [3].

Moment invariants were firstly introduced to the pattern recognition community in 1962 by Hu [4], who employed the results of the theory of algebraic invariants and derived his seven famous invariants to rotation of 2-D objects. Since that time, numerous works have been devoted to various improvements and generalizations of Hu's invariants and also to its use in many application areas.

Dudani [5] and Belkasim [6] described their application to aircraft silhouette recognition, Wong and Hall [7], Goshtasby [8] and Flusser and Suk [9] employed moment invariants in template matching and registration of satellite images, Mukundan [10], [11] applied them to estimate the position and the attitude of the object in 3-D space, Sluzek [12] proposed to use local moment invariants in industrial quality inspection and many authors used moment invariants for character recognition [6], [13], [14], [15], [16]. Maitra [17] and Hupkens [18] made them invariant also to contrast changes, Wang [19] proposed illumination invariants particularly suitable for texture classification. Li [20] and Wong [21] presented the systems of invariants up to the orders nine and five, respectively. Unfortunately, no one of them paid attention to mutual dependence/independence of the invariants. The invariant sets presented in their papers are algebraically dependent. Most recently, Flusser [22], [23] has proposed a method how to derive independent sets of invariants of any orders.

There is also a group of papers [15], [24] and [25] that use *Zernike moments* to construct rotation invariants. Their motivation comes from the fact that Zernike polynomials are orthogonal on a unit circle. Thus, Zernike moments do not contain any redundant information and are more convenient for image reconstruction. However, Teague [24] showed that Zernike invariants of 2nd and 3rd orders are equivalent to Hu's ones when expressing them in terms of geometric moments. He presented the invariants up to eight order in explicit form but no general rule how to derive them is given. Wallin [25] described an algorithm for a formation of moment invariants of any order. Since Teague

[1]This fundamental book contains original notes of the course held by Hilbert in 1897 in Gottingen and was firstly published 50 years after Hilbert's death.

[24] as well as Wallin [25] were particularly interested in reconstruction abilities of the invariants, they didn't pay much attention to the question of independence.

Flusser and Suk [26] and Reiss [27] contributed significantly to the theory of moment invariants by correcting the Fundamental Theorem and deriving invariants to general affine transform.

Several papers studied recognitive and reconstruction aspects, noise tolerance and other numerical properties of various kinds of moment invariants and compared their performance experimentally [6], [28], [29], [30], [31], [32], [33]. Moment invariants were shown to be also a useful tool for geometric normalization of an image [34], [35]. Large amount of effort has been spent to find effective algorithms for moment calculation (see [36] for a survey).

All the above mentioned invariants deal with geometric distortion of the objects. Much less attention has been paid to invariants with respect to changes of the image intensity function (we call them radiometric invariants) and to combined radiometric-geometric invariants. In fact, just the invariants both to radiometric and geometric image degradations are necessary to resolve practical object recognition tasks because usually both types of degradations are present in input images.

Van Gool et al. introduced so-called affine-photometric invariants of graylevel [37] and color [38] images. These features are invariant to the affine transform and to the change of contrast and brightness of the image simultaneously. A pioneer work on this field was done by Flusser and Suk [39] who derived invariants to convolution with an arbitrary centrosymmetric PSF. From the geometric point of view, their descriptors were invariant to translation only. Despite of this, the invariants have found successful applications in face recognition on out-of-focused photographs [40], in normalizing blurred images into the canonical forms [41], [42], in template-to-scene matching of satellite images [39], in blurred digit and character recognition [43], [19], in registration of images obtained by digital subtraction angiography [44] and in focus/defocus quantitative measurement [45]. Other sets of blur invariants (but still only shift-invariant) were proposed for some particular kinds of PSF -– axisymmetric blur invariants [46] and motion blur invariants [47], [48]. A significant improvement motivated by a problem of registration of blurred images was made by Flusser et al. They introduced so-called combined blur-rotation invariants [49] and combined blur-affine invariants [50] and reported their successful usage in satellite image registration [51] and in camera motion estimation [52].

In comparison with a huge number of papers on 2-D moment invariants, only few papers on 3-D and/or even $N$-D invariants have been published. The first attempt to extend 2-D moment invariants to 3-D was done by Sadjadi and Hall [53]. Probably the first systematic approach to derivation of 3-D moment invariants to rotation was published by Lo and Don [54]. It was based on group representation theory. Their results were later rediscovered (with some modifications) by Guo [55] and Galvez and Canton [56]. The Guo's paper derived only three invariants without any possibility of their further extension. There have been several papers trying to generalize 3-D rotational moment

invariants either in the sense of the transformation group and/or in the sense of dimension. Reiss [57] used tensor algebra to derive 3-D moment invariants to affine transform. He showed the invariants published in [53], [54] are just special cases of his descriptors. Another approach to deriving 3-D affine invariants can be found in [58]. Markandey and deFigueiredo [59] tried to extend moment invariants to dimensions greater than three. They used the fundamental theorem from the classical paper [4]. As it was pointed out by Mamistvalov [60] and later by Reiss [27], this theorem contained some errors. However, these errors were incorporated also into [59]. Finally, Mamistvalov [61] published the correct version of the fundamental theorem of moment invariants in arbitrary dimensions and showed how to use it to derive $N$-D affine moment invariants (it should be pointed out that a shorter version of this paper was published by the same author in a local journal 24 years earlier [62]). Most recently, Flusser et al. proposed an extension of the blur moment invariants [63] and the combined blur-rotation invariants into 3-D [64].

# 3 Basic Terms

First we define basic terms which will be then used in the construction of the invariants.

**Definition 1:** By *image function* (or *image*) we understand any real function $f(x, y)$ having a bounded support and a finite nonzero integral.

**Definition 2:** *Geometric moment* $m_{pq}$ of image $f(x, y)$, where $p, q$ are non-negative integers and $(p + q)$ is called the *order* of the moment, is defined as

$$m_{pq} = \int_{-\infty}^{\infty}\int_{-\infty}^{\infty} x^p y^q f(x, y)\mathrm{d}x\mathrm{d}y. \tag{2}$$

Corresponding *central moment* $\mu_{pq}$ and *normalized moment* $\nu_{pq}$ are defined as

$$\mu_{pq} = \int_{-\infty}^{\infty}\int_{-\infty}^{\infty} (x - x_c)^p (y - y_c)^q f(x, y)dxdy, \tag{3}$$

$$\nu_{pq} = \frac{\mu_{pq}}{\mu_{00}^{\omega}}, \tag{4}$$

respectively, where the coordinates $(x_c, y_c)$ denote the centroid of $f(x, y)$, and $\omega = (p + q + 2)/2$.

**Definition 3:** *Complex moment* $c_{pq}$ of image $f(x, y)$ is defined as

$$c_{pq} = \int_{-\infty}^{\infty}\int_{-\infty}^{\infty} (x + iy)^p (x - iy)^q f(x, y)dxdy \tag{5}$$

where $i$ denotes imaginary unit. Definitions of central and normalized complex moments are analogous to (3) and (4).

Geometric moments and complex moments carry the same amount of information. Each complex moment can be expressed in terms of geometric moments as

$$c_{pq} = \sum_{k=0}^{p}\sum_{j=0}^{q} \binom{p}{k}\binom{q}{j} (-1)^{q-j} \cdot i^{p+q-k-j} \cdot m_{k+j,p+q-k-j} \tag{6}$$

and vice versa:

$$m_{pq} = \frac{1}{2^{p+q} i^q} \sum_{k=0}^{p} \sum_{j=0}^{q} \binom{p}{k} \binom{q}{j} (-1)^{q-j} \cdot c_{k+j,p+q-k-j}. \tag{7}$$

The reason for introducing complex moments is in their favorable behavior under image rotation, as will be shown later.

# 4 Invariants to rotation, translation, and scaling

Invariants to similarity transformation group were the first invariants that appeared in pattern recognition literature. It was caused partly because of their simplicity, partly because of great demand for invariant features that could be used in position-independent object classification. In this problem formulation, degradation operator $\mathcal{D}$ is supposed to act solely in spatial domain and to have a form of similarity transform. Eq (1) then reduces to

$$g(\tau(x, y)) = f(x, y), \tag{8}$$

where $\tau(x, y)$ denotes arbitrary rotation, translation, and scaling.

Invariants to translation and scaling are trivial – central and normalized moments themselves can play this role. As early as in 1962, M.K. Hu [4] published seven rotation invariants, consisting of second and third order moments:

$$\begin{aligned}
\phi_1 &= \mu_{20} + \mu_{02}, \\
\phi_2 &= (\mu_{20} - \mu_{02})^2 + 4\mu_{11}^2, \\
\phi_3 &= (\mu_{30} - 3\mu_{12})^2 + (3\mu_{21} - \mu_{03})^2, \\
\phi_4 &= (\mu_{30} + \mu_{12})^2 + (\mu_{21} + \mu_{03})^2, \\
\phi_5 &= (\mu_{30} - 3\mu_{12})(\mu_{30} + \mu_{12})((\mu_{30} + \mu_{12})^2 - 3(\mu_{21} + \mu_{03})^2) + \\
&\quad (3\mu_{21} - \mu_{03})(\mu_{21} + \mu_{03})(3(\mu_{30} + \mu_{12})^2 - (\mu_{21} + \mu_{03})^2), \\
\phi_6 &= (\mu_{20} - \mu_{02})((\mu_{30} + \mu_{12})^2 - (\mu_{21} + \mu_{03})^2) + 4\mu_{11}(\mu_{30} + \mu_{12})(\mu_{21} + \mu_{03}), \\
\phi_7 &= (3\mu_{21} - \mu_{03})(\mu_{30} + \mu_{12})((\mu_{30} + \mu_{12})^2 - 3(\mu_{21} + \mu_{03})^2) - \\
&\quad (\mu_{30} - 3\mu_{12})(\mu_{21} + \mu_{03})(3(\mu_{30} + \mu_{12})^2 - (\mu_{21} + \mu_{03})^2).
\end{aligned} \tag{9}$$

The Hu's invariants became classical and, despite of their drawbacks, they have found numerous successful applications in various areas. Major weakness of the Hu's theory is that it does not provide for a possibility of any generalization. By means of it, we could not derive invariants from higher-order moments and invariants to more general transformations. These limitations were overcome thirty years later.

After Hu, there have been published various approaches to the theoretical derivation of moment-based rotation invariants. Li [20] used Fourier-Mellin transform, Teague [24] and Wallin [25] proposed to use Zernike moments and Wong [21] used complex monomials which originate from the theory of algebraic invariants. Here, we present a scheme introduced by Flusser [22], [23], which is based on the complex moments. The idea to

use the complex moments for deriving invariants was firstly proposed by Mostafa and Psaltis [30] but they focused on the evaluation of the invariants rather than on constructing higher-order systems. In comparison with the previous approaches, our approach is more transparent and allows to study mutual dependence/independence of the invariants easily. It should be noted that all the above approaches differ from each other formally by mathematical tools and notation used but the general idea behind them is common and the results are similar or even equivalent.

In polar coordinates, (5) becomes the form

$$c_{pq} = \int_0^{\infty} \int_0^{2\pi} r^{p+q+1} e^{i(p-q)\theta} f(r,\theta) dr d\theta. \tag{10}$$

It follows from the definition that $c_{pq} = c_{qp}^*$ (the asterisk denotes complex conjugate). Furthermore, it follows immediately from (10) that the moment magnitude $|c_{pq}|$ is invariant to rotation of the image while the phase is shifted by $(p-q)\alpha$, where $\alpha$ is the angle of rotation. More precisely, it holds for the moment of the rotated image

$$c'_{pq} = e^{-i(p-q)\alpha} \cdot c_{pq}. \tag{11}$$

Any approach to the construction of rotation invariants is based on a proper kind of phase cancellation. The simplest method proposed by many authors is to use the moment magnitudes themselves as the invariants. However, they do not generate a complete set of invariants. In the following Theorem, phase cancellation is achieved by multiplication of appropriate moment powers.

**Theorem 1:** Let $n \geq 1$ and let $k_i, p_i$, and $q_i$ $(i = 1, \cdots, n)$ be non-negative integers such that

$$\sum_{i=1}^{n} k_i(p_i - q_i) = 0.$$

Then

$$I = \prod_{i=1}^{n} c_{p_i q_i}^{k_i} \tag{12}$$

is invariant to rotation.

According to Theorem 1, some simple examples of rotation invariants are $c_{11}, c_{20}c_{02}, c_{20}c_{12}^2$, etc. As a rule, most invariants (12) are complex. If we want to have real-valued features, we only take real and imaginary parts of each of them. To achieve also translation invariance, we use central coordinates in the definition of the complex moments (5).

Theorem 1 allows us to construct an infinite number of the invariants for any order of moments, but only few of them are mutually independent. By the term *basis* we intuitively understand the smallest set by means of which all other invariants can be expressed. The knowledge of the basis is a crucial point in all pattern recognition problems because dependent features do not contribute to the discrimination power of the system at all and may even cause object misclassifications due to the "curse of dimensionality". For instance, the set

$$\{c_{20}c_{02}, c_{21}^2 c_{02}, c_{12}^2 c_{20}, c_{21}c_{12}, c_{21}^3 c_{02}c_{12}\}$$

is a dependent set whose basis is $\{c_{12}^2 c_{20}, c_{21} c_{12}, \}$.

Fundamental theorem on how to construct an invariant basis for a given set of moments was firstly formulated and proven in [22] and later in more general form (which is shown below) in [23].

**Theorem 2:** Let us consider complex moments up to the order $r \geq 2$. Let a set of rotation invariants $\mathcal{B}$ be constructed as follows:

$$(\forall p, q | p \geq q \wedge p + q \leq r)(\Phi(p, q) \equiv c_{pq} c_{q_0 p_0}^{p-q} \in \mathcal{B}),$$

where $p_0$ and $q_0$ are arbitrary indices such that $p_0 + q_0 \leq r$, $p_0 - q_0 = 1$ and $c_{p_0 q_0} \neq 0$ for all images involved. Then $\mathcal{B}$ is a basis of a set of all rotation invariants created from the moments up to the order $r$.

Theorem 2 is very strong because it claims $\mathcal{B}$ is a basis of *all possible* rotation invariants, not only of those constructed according to (12). We can even show that, knowing the basis $\mathcal{B}$, it is possible to reconstruct the original object with theoretically unlimited accuracy.

**Example:** The basis of the invariants composed of the moments of 2nd and 3rd orders, which was constructed according to Theorem 2 by choosing $p_0 = 2$ and $q_0 = 1$.

$$\begin{aligned} \Phi(1,1) &= c_{11}, \\ \Phi(2,1) &= c_{21} c_{12}, \\ \Phi(2,0) &= c_{20} c_{12}^2, \\ \Phi(3,0) &= c_{30} c_{12}^3. \end{aligned} \tag{13}$$

Theorem 2 has a very surprising consequence. We can prove that, contrary to common belief, the Hu's system is dependent and incomplete, so in fact it does not form a good feature set. The same is true for invariant sets proposed by Li [20] and Wong [21]. This result firstly appeared in [22] and has a deep practical impact.

# 5 Invariants to affine transform

In practice we often face object deformations that are beyond the rotation-translation-scaling model. An exact model of photographing a planar scene by a pin-hole camera whose optical axis is not perpendicular to the scene is *projective transform* of spatial coordinates. Since the projective transform is not linear, its Jacobian is a function of spatial coordinates and projective moment invariants from a finite number of moments cannot exist [66, 67].

For small objects and large camera-to-scene distance is the perspective effect negligible and the projective transform can be well approximated by *affine transform*

$$\begin{aligned} x' &= a_0 + a_1 x + a_2 y, \\ y' &= b_0 + b_1 x + b_2 y. \end{aligned} \tag{14}$$

Thus, having powerful affine moment invariants for object description and recognition is in great demand.

A pioneer work on this field was done independently by Reiss [27] and Flusser and Suk [26], [65], who introduced affine moment invariants (AMI's) and proved their applicability in simple recognition tasks. They derived only few invariants in explicit forms and they did not study the problem of their mutual independence.

Here we present a new general method how to systematically derive arbitrary number of the AMI's of any weights and any orders, This method is based on representation of the AMI's by graphs.

Let us consider an image $f$ and two arbitrary points $(x_1, y_1)$, $(x_2, y_2)$ from its support. Let us denote the "cross-product" of these points as $T_{12}$:

$$T_{12} = x_1 y_2 - x_2 y_1.$$

After an affine transform it holds $T'_{12} = J \cdot T_{12}$, where $J$ is the Jacobian of the transform. The basic idea of the AMI's generating is the following. We consider various numbers of points and we integrate their cross-products (or some powers of their cross-products) on the support of $f$. These integrals can be expressed in terms of moments and, after eliminating the Jacobian by proper normalization, they yield affine invariants.

More precisely, having $N$ points ($N \geq 2$) we define functional $I$ depending on $N$ and on non-negative integers $n_{kj}$ as

$$I(f) = \int_{-\infty}^{\infty} \prod_{k,j=1}^{N} T_{kj}^{n_{kj}} \cdot \prod_{i=1}^{N} f(x_i, y_i) dx_i dy_i. \tag{15}$$

Note that it is meaningful to consider only $j > k$, because $T_{kj} = -T_{jk}$ and $T_{kk} = 0$. After an affine transform, $I$ becomes

$$I' = J^w |J|^N \cdot I,$$

where $w = \sum_{k,j} n_{kj}$ is called the *weight* of the invariant and $N$ is called the *degree* of the invariant.

If $I$ is normalized by $\mu_{00}^{w+N}$ we get a desirable affine invariant

$$\left(\frac{I}{\mu_{00}^{w+N}}\right)' = \left(\frac{I}{\mu_{00}^{w+N}}\right)$$

(if $w$ is odd and $J < 0$ there is an additional factor $-1$).

We illustrate the general formula (15) on two simple invariants. First, let $N = 2$ and $n_{12} = 2$. Then

$$I(f) = \int_{-\infty}^{\infty} (x_1 y_2 - x_2 y_1)^2 f(x_1, y_1) f(x_2, y_2) dx_1 dy_1 dx_2 dy_2 = 2(m_{20} m_{02} - m_{11}^2). \tag{16}$$

Similarly, for $N = 3$ and $n_{12} = 2, n_{13} = 2, n_{23} = 0$ we get

$$
\begin{aligned}
I(f) &= \int_{-\infty}^{\infty} (x_1y_2 - x_2y_1)^2(x_1y_3 - x_3y_1)^2 f(x_1,y_1)f(x_2,y_2)f(x_3,y_3)dx_1dy_1dx_2dy_2dx_3dy_3 \\
&= m_{20}^2 m_{04} - 4m_{20}m_{11}m_{13} + 2m_{20}m_{02}m_{22} + 4m_{11}^2 m_{22} \\
&\quad -4m_{11}m_{02}m_{31} + m_{02}^2 m_{40}. \qquad (17)
\end{aligned}
$$

The above idea has an analogy in graph theory. Each invariant generated by formula (15) can be represented by a graph, where each point $(x_k, y_k)$ corresponds to one node and each cross-product $T_{kj}$ corresponds to one edge of the graph. If $n_{kj} > 1$, the respective term $T_{kj}^{n_{kj}}$ corresponds to $n_{kj}$ edges connecting $k$-th and $j$-th nodes. Thus, the number of nodes equals the degree of the invariant and the total number of the graph edges equals the weight $w$ of the invariant. From the graph one can also learn about the orders of the moments the invariant is composed of and about its structure. The number of edges originating from each node equals the order of the moments involved. Each invariant of the form (15) is in fact a sum where each term is a product of certain number of moments. This number is constant for all terms of one invariant and is equal to the total number of the graph nodes. Particularly, for the invariants (16) and (17) the corresponding graphs are shown in Fig. 4.

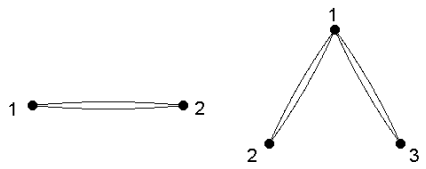


Figure 4: The graphs corresponding to the invariants (16) (left) and (17) (right)

Now one can see that the problem of derivation of the AMI's up to the given weight $w$ is equivalent to generating all graphs with at least two nodes and at most $w$ edges. This is a combinatorial task with exponential complexity but formally easy to implement. Unfortunately, most resulting graphs are useless because they generate invariants, which are dependent. Identifying and discarding them is very important but very complicated task.

There might be various kinds of dependencies in the set of all AMI's (i.e. in the set of all graphs). The invariant which equals to linear combinations of other invariants or of products of other invariants is called *reducible* invariant. Other invariants than reducible are called *irreducible* invariants. Unfortunately, "irreducible" does not mean "independent" – there may be higher-order polynomial dependencies among irreducible invariants. Current methods [68] perfectly eliminate reducible invariants but identification of dependencies among irreducible invariants has not been resolved yet.

For illustration, let us consider AMI's up to the weight 10. Using the graph method we got, after discarding isomorphic graphs, 1519 AMI's in explicit forms. Then we applied the algorithms eliminating reducible invariants, which led to 362 irreducible invariants.

# 6 Invariants to convolution

Two previous sections were devoted to the invariants with respect to transformation of spatial coordinates only. Now let us consider an imaging system with ideal geometry, i.e. $\tau(x, y) = (x, y)$, but suffering from non-ideal optical/radiometrical properties. Assuming the system is shift invariant, degradation operator $\mathcal{D}$ has a form of

$$g(x, y) = (f * h)(x, y), \tag{18}$$

where $h(x, y)$ is the point-spread function (PSF) of the system. This is a simple but realistic model of degradations introduced by out-of-focused camera ($h(x, y)$ has then a cylindrical shape), by camera and/or scene motion ($h(x, y)$ has a form of rectangular pulse), and by photographing through turbulent medium ($h(x, y)$ is then a Gaussian), to name a few. However, in real applications the PSF has more complex form because it use to be a composition of several degradation factors. Neither the shape nor the parameters of the PSF use to be known. This high-level uncertainty prevents us from solving eq. (18) as an inverse problem. Although such attempts were published (see [69] or [70] for a basic survey), they did not yield satisfactory results.

In this section, we present functionals invariant to convolution with arbitrary centrosymmetric PSF (in image analysis literature they are often called "blur invariants" because common PSF's have a character of a low-pass filter). Blur invariants were firstly introduced by Flusser and Suk [39]. They have found successful applications in face recognition on out-of-focused photographs [40], in normalizing blurred images into the canonical forms [41], [42], in template-to-scene matching of satellite images [39], in blurred digit and character recognition [43], [19], in registration of images obtained by digital subtraction angiography [44] and in focus/defocus quantitative measurement [45].

The assumption of centrosymmetry is not a significant limitation of practical utilization of the method. Most real sensors and imaging systems, both optical and non-optical ones, have the PSF with certain degree of symmetry. In many cases they have even higher symmetry than the central one, such as axial or radial symmetry.

Principal theorem on convolution invariants is the following.

**Theorem 3:** Let functional $C : L_1(R^2) \times \mathbf{N_0} \times \mathbf{N_0} \to \mathbf{R}$ be defined as follows:
If $(p + q)$ is even then

$$C(p, q)^{(f)} = 0.$$

If $(p + q)$ is odd then

$$C(p, q)^{(f)} = \mu_{pq}^{(f)} - \frac{1}{\mu_{00}^{(f)}} \sum_{n=0}^{p} \sum_{\substack{m=0 \\ 0<n+m<p+q}}^{q} \binom{p}{n} \binom{q}{m} C(p-n, q-m)^{(f)} \cdot \mu_{nm}^{(f)}. \tag{19}$$

Then

$$C(p, q)^{(f*h)} = C(p, q)^{(f)}$$

for any image function $f$, any non-negative integers $p$ and $q$, and for any centrosymmetric PSF $h$.

Theorem 3 tells that blur invariants are recursively defined functionals consisting mainly from odd-order moments. Although they do not have straightforward "physical" interpretation, let us make a few notes to provide a better insight into their meaning. Any invariant (even different from those presented here) to convolution with a centrosymmetric PSF must give a constant response on centrosymmetric images. This is because any centrosymmetric image can be considered as a blurring PSF acting on delta-function. It can be proven that if $f$ is centrosymmetric then $C(p,q)^{(f)} = 0$ for any $p$ and $q$. The opposite implication is valid as well. Thus, what image properties are reflected by the $C(p,q)$'s? Let us consider a Fourier-based decomposition $f = f_c + f_a$ where $f_c$, $f_a$ are centrosymmetric and antisymmetric components of $f$, respectively. Function $f_a$ can be exactly recovered from odd-order moments of $f$ (while even-order moments of $f_a$ equal zero) and vice versa. A similar relation holds for the invariants $C(p,q)$. Thus, all $C(p,q)$'s reflect mainly properties of the antisymmetric component of the image, while all symmetric images are in their null-space.

Blur invariants introduced in Theorem 3 have also a close relationship to the Fourier transform of the image. Since $h(x,y)$ is supposed to be centrosymmetric, the phases of $F(u,v)$ and $G(u,v)$ can differ from one another only by 0 or $\pi$. Thus, tangent of the phase is blur invariant. It can be shown that tangent of the Fourier transform phase can be expanded into power series, whose coefficient at monomial $u^p v^q$ equals the functional $C(p,q)$ (for proofs and detailed discussion see [39]).

For illustration, below we show a set of invariants of the 3rd, 5th and 7th orders in explicit forms.

- 3rd order:

$$C(3,0) = \mu_{30},$$
$$C(2,1) = \mu_{21},$$
$$C(1,2) = \mu_{12},$$
$$C(0,3) = \mu_{03}.$$

- 5th order:

$$C(5,0) = \mu_{50} - \frac{10\mu_{30}\mu_{20}}{\mu_{00}},$$
$$C(4,1) = \mu_{41} - \frac{2}{\mu_{00}}(3\mu_{21}\mu_{20} + 2\mu_{30}\mu_{11}),$$
$$C(3,2) = \mu_{32} - \frac{1}{\mu_{00}}(3\mu_{12}\mu_{20} + \mu_{30}\mu_{02} + 6\mu_{21}\mu_{11}),$$
$$C(2,3) = \mu_{23} - \frac{1}{\mu_{00}}(3\mu_{21}\mu_{02} + \mu_{03}\mu_{20} + 6\mu_{12}\mu_{11}),$$
$$C(1,4) = \mu_{14} - \frac{2}{\mu_{00}}(3\mu_{12}\mu_{02} + 2\mu_{03}\mu_{11}),$$

$$C(0,5) = \mu_{05} - \frac{10\mu_{03}\mu_{02}}{\mu_{00}}.$$

- 7th order:

$$C(7,0) = \mu_{70} - \frac{7}{\mu_{00}}(3\mu_{50}\mu_{20} + 5\mu_{30}\mu_{40}) + \frac{210\mu_{30}\mu_{20}^2}{\mu_{00}^2},$$

$$C(6,1) = \mu_{61} - \frac{1}{\mu_{00}}(6\mu_{50}\mu_{11} + 15\mu_{41}\mu_{20} + 15\mu_{40}\mu_{21} + 20\mu_{31}\mu_{30}) + \\ + \frac{30}{\mu_{00}^2}(3\mu_{21}\mu_{20}^2 + 4\mu_{30}\mu_{20}\mu_{11}),$$

$$C(5,2) = \mu_{52} - \frac{1}{\mu_{00}}(\mu_{50}\mu_{02} + 10\mu_{30}\mu_{22} + 10\mu_{32}\mu_{20} + 20\mu_{31}\mu_{21} + 10\mu_{41}\mu_{11} + 5\mu_{40}\mu_{12}) + \\ + \frac{10}{\mu_{00}^2}(3\mu_{12}\mu_{20}^2 + 2\mu_{30}\mu_{20}\mu_{02} + 4\mu_{30}\mu_{11}^2 + 12\mu_{21}\mu_{20}\mu_{11}),$$

$$C(4,3) = \mu_{43} - \frac{1}{\mu_{00}}(\mu_{40}\mu_{03} + 18\mu_{21}\mu_{22} + 12\mu_{31}\mu_{12} + 4\mu_{30}\mu_{13} + 3\mu_{41}\mu_{02} + 12\mu_{32}\mu_{11} + 6\mu_{23}\mu_{20}) + \\ + \frac{6}{\mu_{00}^2}(\mu_{03}\mu_{20}^2 + 4\mu_{30}\mu_{11}\mu_{02} + 12\mu_{21}\mu_{11}^2 + 12\mu_{12}\mu_{20}\mu_{11} + 6\mu_{21}\mu_{02}\mu_{20}),$$

$$C(3,4) = \mu_{34} - \frac{1}{\mu_{00}}(\mu_{04}\mu_{30} + 18\mu_{12}\mu_{22} + 12\mu_{13}\mu_{21} + 4\mu_{03}\mu_{31} + 3\mu_{14}\mu_{20} + 12\mu_{23}\mu_{11} + 6\mu_{32}\mu_{02}) + \\ + \frac{6}{\mu_{00}^2}(\mu_{30}\mu_{02}^2 + 4\mu_{03}\mu_{11}\mu_{20} + 12\mu_{12}\mu_{11}^2 + 12\mu_{21}\mu_{02}\mu_{11} + 6\mu_{12}\mu_{20}\mu_{02}),$$

$$C(2,5) = \mu_{25} - \frac{1}{\mu_{00}}(\mu_{05}\mu_{20} + 10\mu_{03}\mu_{22} + 10\mu_{23}\mu_{02} + 20\mu_{13}\mu_{12} + 10\mu_{14}\mu_{11} + 5\mu_{04}\mu_{21}) + \\ + \frac{10}{\mu_{00}^2}(3\mu_{21}\mu_{02}^2 + 2\mu_{03}\mu_{02}\mu_{20} + 4\mu_{03}\mu_{11}^2 + 12\mu_{12}\mu_{02}\mu_{11}),$$

$$C(1,6) = \mu_{16} - \frac{1}{\mu_{00}}(6\mu_{05}\mu_{11} + 15\mu_{14}\mu_{02} + 15\mu_{04}\mu_{12} + 20\mu_{13}\mu_{03}) + \\ + \frac{30}{\mu_{00}^2}(3\mu_{12}\mu_{02}^2 + 4\mu_{03}\mu_{02}\mu_{11}),$$

$$C(0,7) = \mu_{07} - \frac{7}{\mu_{00}}(3\mu_{05}\mu_{02} + 5\mu_{03}\mu_{04}) + \frac{210\mu_{03}\mu_{02}^2}{\mu_{00}^2}.$$

It should be noted that similar invariant functionals can be constructed when the PSF is supposed to have some other type of symmetry, like axial symmetry, four-fold symmetry, or circular symmetry [46], [47], [40]. Generally, the stronger the symmetry assumptions, the more invariants exist and the less functions is contained in their null-space. On the other hand, if the PSF has no symmetry, then there exists only one invariant $\mu_{00}$.

# 7 Combined invariants

In this section, we describe so-called *combined invariants* that are invariant simultaneously to convolution and transformation of spatial coordinates.

We assume the degradation model (1) where $\tau$ is restricted to group of linear transformations and $h$ is supposed to have certain degree of symmetry. Combined invariants are very important for practical purposes because usually both types of degradations – geometric as well as radiometric – are present in input images.

The history of combined invariants is very short. First, combined blur-rotation invariants were introduced by Zitova and Flusser [49], who also reported their successful usage in satellite image registration [51] and in camera motion estimation [52]. Later on, blur-rotation invariants were extended into 3-D and their application to template matching in magnetic resonance images (MRI) were described [64]. Most recently, Suk and Flusser derived combined invariants to convolution and affine transform [50].

Roughly speaking, combined invariants are constructed by substitution of blur invariants in place of moments when constructing geometric invariants, and vice versa. There are several ways how to perform the substitution. The most general approach is expressed in the following principal theorem (for its proof see [50]).

**Theorem 4:** Let $I(\mu_{00}, \cdots, \mu_{PQ})$ be an affine moment invariant. Then $I(C(0,0), \cdots, C(P,Q))$, where functionals $C(p,q)$ are defined in Theorem 3, is a combined blur-affine invariant.

# 8 Orthogonal moments

It is well known from linear algebra that an orthogonal basis of a vector space have many favorable properties comparing to other bases. They are, of course, theoretically equivalent, because each vector from one basis can be expressed as a linear combination of vectors from other basis. From practical point of view, when reconstructing a vector from only few basic projections, orthogonal basis provides us usually with much more accurate reconstruction than other bases. Reconstruction problem was the main motivation (although not the only one) of introducing orthogonal moments into pattern recognition community [15], [24], [25], [71].

By *orthogonal moment* $M_{pq}$ we understand projection of image function $f$ onto a set of orthogonal polynomials $\{\mathcal{P}_{pq}(x,y)\}$, i.e.

$$M_{pq} = \int\int \mathcal{P}_{pq}(x,y) f(x,y) dx dy.$$

In addition to its efficiency, image reconstruction from orthogonal moments is very simple. While the reconstruction from geometric moments must be carried out in Fourier domain using Taylor's expansion of $F$

$$F(u,v) = \sum_p \sum_q \frac{(-2\pi i)^{p+q}}{p!q!} m_{pq} u^p v^q,$$

reconstruction from orthogonal moments is performed directly in the image domain

$$f(x,y) = \sum_p \sum_q M_{pq} \mathcal{P}_{pq}(x,y).$$

The most popular sets of orthogonal polynomials used for moment construction are Legendre, Zernike, and Czebychev polynomials.

## 8.1 Legendre polynomials and moments

One-dimensional Legendre polynomial of order $n$ is defined as

$$P_n(x) = \frac{1}{2^n n!} \frac{\partial^n}{\partial x^n}(x^2-1)^n,$$

where $|x| \leq 1$.

Legendre polynomials form an orthogonal basis of the polynomial space, because

$$\int_{-1}^{1} P_n(x) P_m(x) dx = \frac{2}{2m+1}\delta_{mn}.$$

First four Legendre polynomials in explicit forms are

$$\begin{aligned} P_0(x) &= 1, \\ P_1(x) &= x, \\ P_2(x) &= \frac{3x^2-1}{2}, \\ P_3(x) &= \frac{5x^3-3x}{2}. \end{aligned}$$

Two-dimensional Legendre moments are then defined as

$$L_{pq} = \frac{(2p+1)(2q+1)}{4} \int_{-1}^{1}\int_{-1}^{1} P_p(x) P_q(y) f(x,y) dxdy.$$

Image reconstruction from Legendre moments is given by

$$f(x,y) = \sum_p \sum_q L_{pq} P_p(x) P_q(y).$$

Since Legendre polynomials are functions of basic monomials $x^p$, Legendre moments can be expressed in terms of geometric moments

$$L_{pq} = \frac{(2p+1)(2q+1)}{4} \sum_{k=0}^{p}\sum_{j=0}^{q} a_{pk} a_{qj} m_{kj},$$

where $a_{pk}$ and $a_{qj}$ are the coefficients. Note that Legendre moment of order $r$ depends only on geometric moments of the same order and of lower orders. For Legendre moments up to the second order we get

$$\begin{aligned} L_{00} &= m_{00}, \\ L_{10} &= \frac{3}{4} m_{00}, \\ L_{20} &= \frac{5}{8}(3m_{20} - m_{00}), \\ L_{11} &= \frac{9}{4} m_{11}. \end{aligned}$$

## 8.2 Zernike polynomials and moments

Two-dimensional Zernike polynomials are defined on a unit circle as

$$V_{nm}(r,\theta) = R_{nm}(r)e^{im\theta},$$

where the radial part

$$R_{nm}(r) = \sum_{k=m}^{n} b_k r^k$$

and $r \leq 1$.

Zernike polynomials fulfill the requirement of orthogonality

$$\int_0^{2\pi}\int_0^1 V_{nj}^*(r,\theta)V_{mk}(r,\theta)rdrd\theta = \frac{\pi}{n+1}\delta_{mn}\delta_{jk}.$$

The radial polynomials themselves are also orthogonal:

$$\int_0^1 R_{nk}(r)R_{mk}(r)rdr = \frac{1}{2(n+1)}\delta_{mn}.$$

Zernike moments are projections of the image onto Zernike polynomials

$$Z_{pq} = \frac{p+1}{\pi}\int_0^{2\pi}\int_0^1 V_{pq}^*(r,\theta)f(r,\theta)rdrd\theta,$$

where $p-|q|$ is even and non-negative.

Image reconstruction formula from Zernike moments is similar to that of Legendre moments

$$f(r,\theta) = \sum_p\sum_q Z_{pq}V_{pq}(r,\theta).$$

Zernike moments have close relationship to complex moments. Recalling the expression of complex moments in polar coordinates (10), it is easy to show that

$$\begin{aligned} Z_{pq} &= \frac{p+1}{\pi}\int_0^{2\pi}\int_0^1 R_{pq}(r)e^{-iq\theta}f(r,\theta)rdrd\theta \\ &= \frac{p+1}{\pi}\sum_{k=q}^{p} b_k \int_0^{2\pi}\int_0^1 r^k e^{-iq\theta}f(r,\theta)rdrd\theta \\ &= \frac{p+1}{\pi}\sum_{k=q}^{p} b_k c_{(k-q)/2,(k+q)/2}. \end{aligned}$$

In particular, we get for low-order Zernike moments

$$\begin{aligned} Z_{00} &= \frac{1}{\pi}m_{00}, \\ Z_{11} &= \frac{2}{\pi}(m_{10} - im_{01}), \\ Z_{20} &= \frac{6}{\pi}(m_{20}+m_{02}) - \frac{3}{\pi}m_{00}. \end{aligned}$$

In the literature, complex moments $c_{(k-q)/2,(k+q)/2}$ are often called Fourier-Mellin moments and denoted as $F_{kq}$.

Zernike moments have the same rotation property as complex moments and can be used to derive invariants to rotation. Again, the basic idea is to cancel the phase shift by multiplying appropriate powers of Zernike moments

$$I = \prod_{j=1}^{n} Z_{p_j q_j}^{k_j} \qquad \sum_{j=1}^{n} k_j q_j = 0.$$

Obviously, rotation invariants generated by Zernike moments are in fact equivalent to those constructed in Section 4 from complex moments.

# 9 Algorithms for moment computation

Since computing complexity of all moment invariants depends almost solely on the computing complexity of geometric moments themselves, we review efficient algorithms for moment calculation in a discrete space. Most of the methods are focused on binary images but there are also a few methods for graylevel images. Basically, moment computation algorithms can be categorized into two groups: decomposition methods and boundary-based methods. The former methods decompose the object into simple areas (squares, rectangles, rows, etc.) whose moments can be calculated easily in $O(1)$ time. The object moment is then given as a sum of moments of all regions. The latter methods calculate object moments just from the boundary, employing Green's theorem or similar technique.

In the discrete case, the integral in the moment definition must be replaced by a summation. The most common way how to do that is to employ the rectangular (i.e. zero-order) method of numeric integration. Then (2) turns to the well-known form

$$m_{pq} = \sum_{x=1}^{N} \sum_{y=1}^{N} x^p y^q f_{ij}, \tag{20}$$

where $N$ is the size of the image and $f_{ij}$ are the grey levels of individual pixels.

Since direct calculation of discrete moments from eq. (20) is time-consuming (it requires $O(pqN^2)$ operations), a large amount of effort has been spent to develop more efficient algorithms.

The first representative of decomposition methods came from Zakaria [72]. The basic idea of his "Delta" method is to decompose the object to the individual rows of pixels. The object moment is then given as a sum of all row moments, which can be easily calculated just from the coordinates of the first and last pixels. Zakaria's method worked for convex shapes only and dealt with moment approximation (20). Dai [73] further extended Zakaria's method and Li [74] generalized it for non-convex shapes. Recently, Spiliotis and Mertzios [75] and Flusser [76] have published advanced modifications of Delta method. Their algorithm employs block-wise object representation instead of the row-wise one. Thanks to this, it works faster than the original version. Sossa et al. [77] proposed morphological decomposition of an image into square blocks. Similarly to Delta method, the moment of the object is then calculated as a sum of moments of all squares. Wu et al. [78] published another decomposition scheme which also leads to square partitions.

They employed a quad-tree decomposition of the image, where the resulting squares are represented by quad-tree leafs.

Boundary-based methods originate either from Green's theorem, which evaluates the double integral over the object by means of single integration along the object boundary, or from polygonal approximation of the object boundary. Li and Shen [79] proposed a method based on Green's theorem in continuous domain. However, their results depend on the choice of the discrete approximation of the boundary and differ from the theoretical values. Jiang and Bunke [80] approximated the object by a polygon first and then they applied the Green's theorem. Thanks to this, they calculated only single integrals along line segments. Unfortunately, due to two-stage approximation, their method produce inaccurate results. Philips [81] proposed to use discrete Green's theorem instead of the continuous one. For convex shapes, his approach leads to the same formulae as the Delta method and it was shown to yield exact moment values. Recently, Yang and Albregtsen [36] have slightly improved the speed of the Philips' method. The methods based on polygonal approximation of the object boundary calculate the moments from the corner points [82], [83]. These methods are efficient only for simple shapes with few corners.

Another approach published in [84] and [85] shows that moment computation can be effectively implemented in parallel processors. Chen [84] proposed a recursive algorithm for a SIMD processor array, Chung [85] presented a constant-time algorithm on reconfigurable meshes.

As it was recently pointed out by Lin [86] and Flusser [76], zero-order approximation used in (20) can be replaced by exact integration of the monomials $x^p y^q$

$$\begin{aligned} m_{pq} &= \sum_{i=1}^{N}\sum_{j=1}^{N} f_{ij} \int\int_{A_{ij}} x^p y^q dxdy = \\ &= \frac{1}{(p+1)(q+1)} \sum_{i=1}^{N}\sum_{j=1}^{N} f_{ij}((i+\frac{1}{2})^{p+1} - (i-\frac{1}{2})^{p+1})((j+\frac{1}{2})^{q+1} - (j-\frac{1}{2})^{q+1}), \end{aligned}$$

where $A_{ij}$ denotes the area of the pixel $(i, j)$. This new formula can be incorporated into almost all methods cited above and leads to more accurate results.

# 10 Applications

In this section, we demonstrate several successful applications of the above described invariant functionals, both on synthetic as well as real data.

## 10.1 Digit recognition

Automatic recognition of printed digits is nowadays considered trivial and many successful intuitive methods have been described. However, classification of digits which are blurred and/or geometrically deformed requires more sophisticated mathematical tools and usually cannot be resolved by standard techniques. Here, we demonstrate digit classification in the space of invariant functionals.

Binary pictures of the size $48 \times 32$ of ten digits $1, 2, \cdots, 9, 0$ were generated (see Fig. 5a). Each of them was deformed by ten affine transforms and every instance was blurred by ten different masks. The parameters of the affine transforms and the convolution masks were generated randomly. This process was repeated four times (which corresponds to four rows of Fig. 5) with different "dispersion" of the parameters and different noise levels. All deformed digits were classified independently by two minimum-distance classifiers – the first one operated in the space of nine affine moment invariants while the second classifier operated in the space of nine corresponding combined invariants.

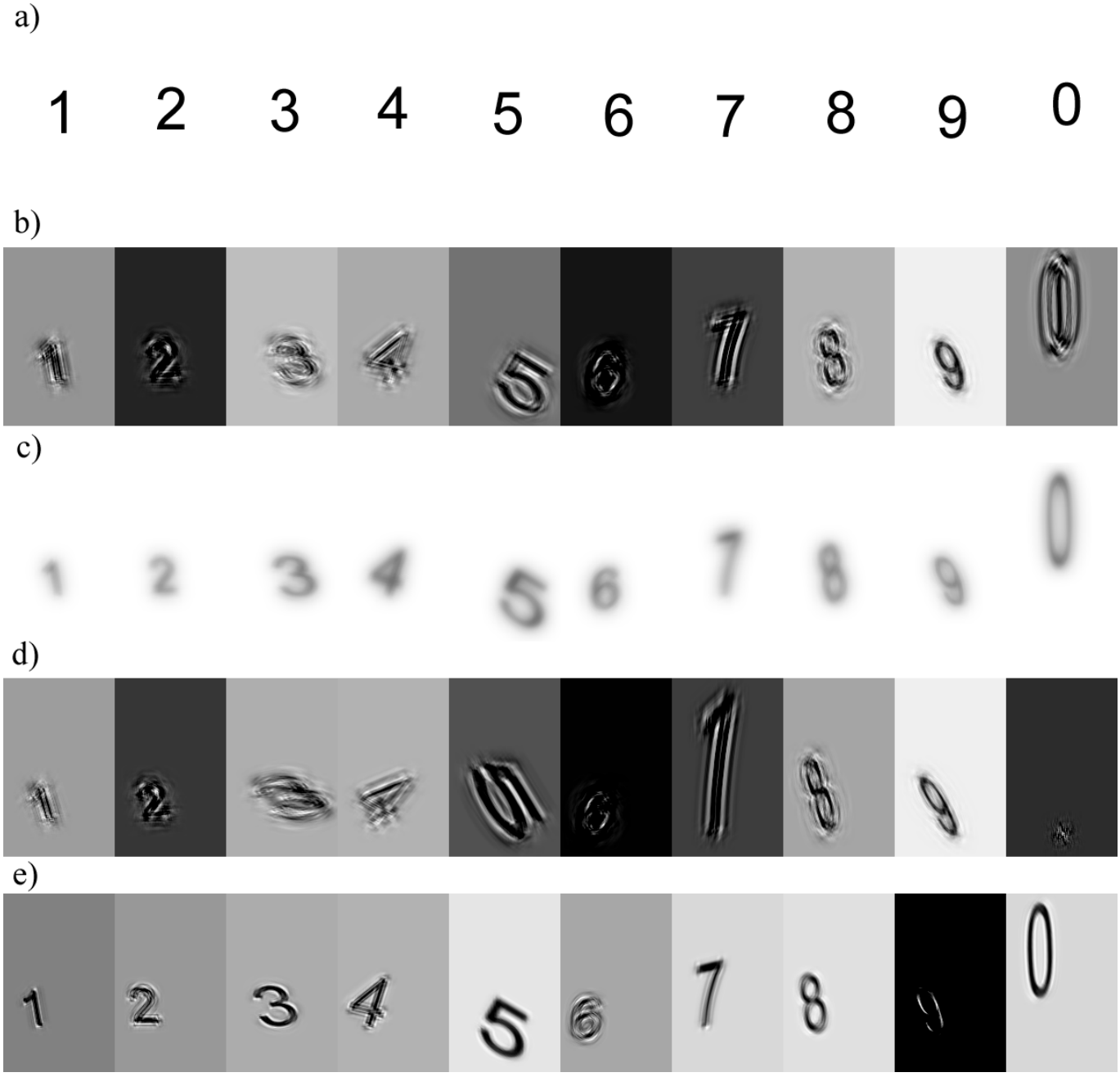


Figure 5: a) Original digits, b)– e) Examples of the deformed digits used in the experiment.

Summarizing the classification results, two important facts are clearly visible. First, the combined invariants yielded an excellent success rate approaching 100%. Second,

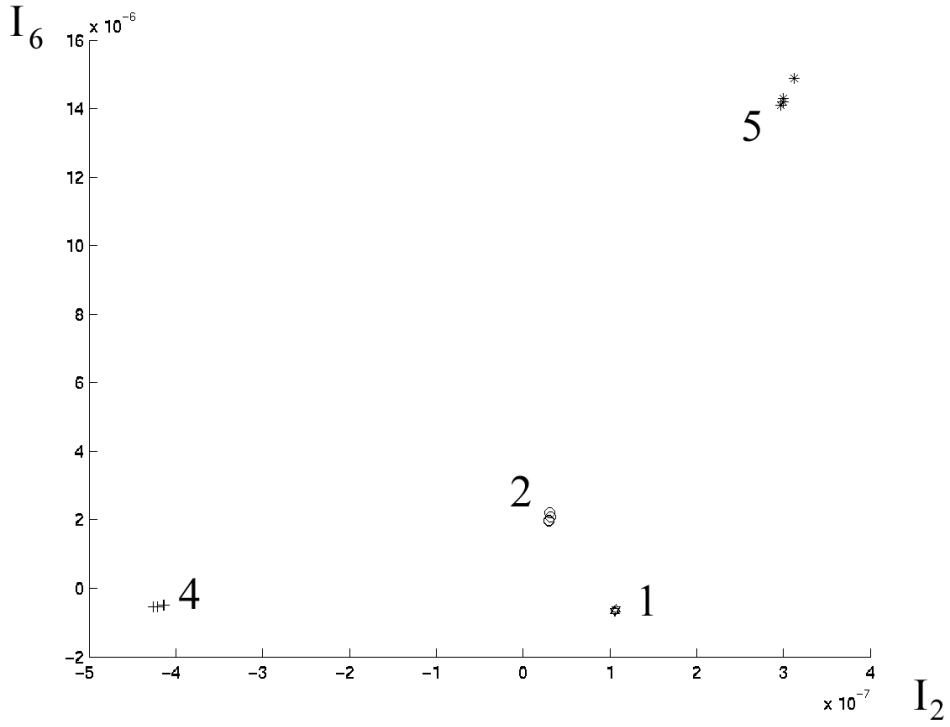


Figure 6: The digits 1, 2, 4, and 5 in the feature space of two combined invariants. Good separability of the classes.

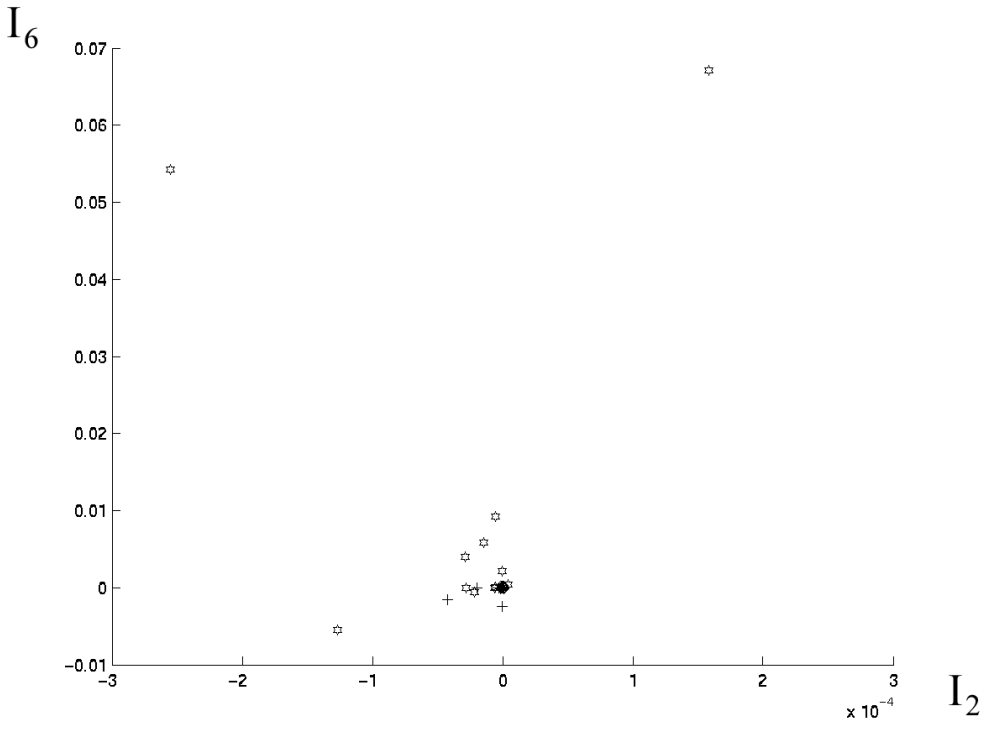


Figure 7: The digits 1, 2, 4, and 5 in the feature space of two affine moment invariants. The classes are not separable because improper invariants were used.

the affine moment invariants perform significantly worse because they cannot handle the blurring properly. A part of the results is graphically visualized in Figs. 6 and 7, where one can see the distribution of digits 1, 2, 4, and 5 in the space of two combined invariants (Fig. 6) and in the space of two corresponding affine moment invariants (Fig. 7). In the space of the combined invariants all digits form compact clusters, well separated from each other. On the contrary, in the space of affine moment invariants all patterns form one bigger cluster and few outliers. The same situation occurs in case of the other digits and can be observed also other feature subspaces. This illustrates that the combined invariants are an actual step toward more robust object recognition and that they significantly improve the recognition rate in case of blurred images.

## 10.2 Camera motion estimation

The problem to be solved is to estimate the motion parameters and the current position of the camera in the real indoor scene. The camera, which takes one frame every second, moves parallel to the wall and rotates. The system monitors the scene and looks for alien objets which may appear in the view of the camera. When such an object appears in front of the camera, the camera is automatically focused on it. Thus, the rest of the scene becomes out-of-focused (see Fig. 8). Position estimation can be resolved via registration of the initial (reference) frame and the image acquired at the moment when the object has appeared. The registration parameters (mutual rotation and shift of the reference and current frames) then unambiguously determine the actual camera position.

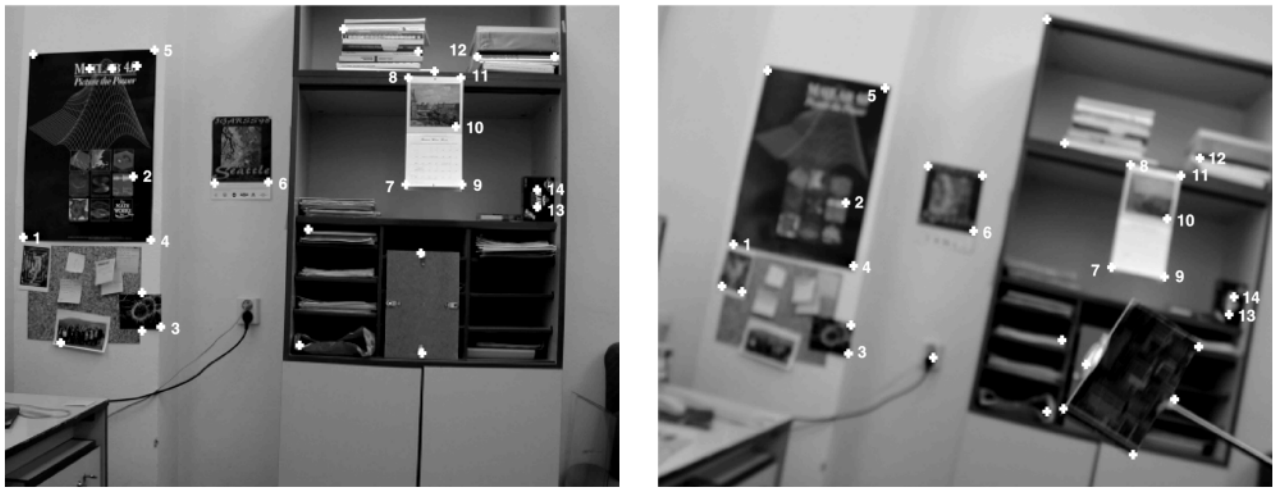


Figure 8: Images of an indoor scene. Camera at the initial position (left); camera at an unknown position, the scene is out-of-focused due to the inserted object (right). 30 CPC's are marked by crosses, those which form the corresponding CP pairs are numbered.

The motion estimation proceeds as follows. First, control point candidates (CPC's) are detected both in the initial and the current frames. Significant corners and other corner-like dominant points are considered as the candidates. To detect them, a method developed particularly for blurred images [90] was employed. In this experiment we de-

tected 30 CPC's in each frame.

Secondly, the correspondence between the CPC's sets must be established and the candidates having no counterparts should be rejected. To do that, a vector of invariants is computed for each CPC over its circular neighborhood (here, three third-order invariants and two fifth-order ones were employed) and then the CPC's are matched in the space of the invariants by minimum-distance rule or by any more sophisticated technique (in this experiment we applied robust matching by means of so-called likelihood coefficients [91]). Once the control point (CP) correspondence is established, their positions can be refined by local search in their neighborhoods. For every pixel from the neighborhood its invariant vector is calculated. The point having the minimum distance to the invariant vector of the CP counterpart is set as the refined position of the CP. If the subpixel accuracy is required, it can be achieved by an appropriate interpolation in the distance matrix.

Finally, as soon as the control point correspondence is established and their coordinates refined, we can find an "optimal" rotational-translational mapping whose parameters are calculated via least-square fit. Knowing these parameters and the initial camera position, the current position can be easily estimated.

We repeated this experiment six times changing the camera rotation and the distance of the inserted object (i.e. the amount of blurring of the background). The results were evaluated by the comparison with ground truth. In all cases the estimates correspond well to the reference values. The errors are mostly below the discretization error. For illustration, in the situation depicted in Fig. 8 the ground-truth registration parameters were rotation $10.92^o$, vertical translation 37.7 pixels, and horizontal translation 41.2 pixels, while the computed parameters were $11.00^o$, 37.7 pixels, and 41.0 pixels, respectively. Summarizing the results of all six experiments, the mean error and standard deviation of the estimation of rotation angle were $0.06^o$ and $0.05^o$, the same for vertical translation were 0.1 and 0.4 pixel, and for horizontal translation 0.3 and 0.5 pixel.

In a comparative experiment, we used exactly the same algorithm but functionals invariant only to rotation were used instead of the combined invariants. None of the six studied cases was correctly resolved. In all cases, many CP pairs were matched incorrectly. For instance, in the experiment in Fig. 8, CP No. 7 was mismatched to the unlabelled CPC to the left from No. 8. This illustrates the actual need of blur invariants when attempting to register blurred images.

## 10.3 Satellite image matching and registration

Motivation of this experiment comes from the area of remote sensing. The template matching problem is usually formulated as follows: having the templates and a digital image of a large scene, one has to find locations of the given templates in the scene. By template we understand a small digital picture usually containing some significant object which was extracted previously from another image of the scene and now is being stored in a database.

There have been proposed numerous image matching techniques in the literature (see the survey paper [92] for instance). A common weakness of all those methods is the assumption that the templates as well as the scene image have been already preprocessed and the degradations like blur, additive noise, etc. have been removed. Those assumptions are not always realistic in practice. For instance, satellite images obtained from Advanced Very High Resolution Radiometer (AVHRR) suffer by blur due to a multiparametric composite PSF of the device [93]. Even if one would know all the parameters (but one usually does not) the restoration would be hard and time-consuming task with an unreliable result. By means of the blur invariants, we can perform the matching without any previous de-blurring.

The experiment was carried out on a simulated AVHRR image. As an input for a simulation, the $512 \times 512$ SPOT HRV image covering the north-western part of Prague was used (see Fig. 9). To simulate AVHRR acquisition, the image was blurred by a $9 \times 13$ mask representing a composite PSF of the AVHRR sensor and corrupted by Gaussian additive noise with standard deviation STD = 10, which yields SNR = 14 in this case (see Fig. 10). The templates were extracted from SPOT image of the same scene and represent significant objects in Prague: the island in Vltava river, the cross of the roads and the soccer stadium (see Fig. 11). The true locations of the templates in the original image are shown in Fig. 9. The task was to localize these templates in the AVHRR image.

Matching of the templates and the AVHRR image was performed by minimum distance in the space of blur invariants and, for a comparison, by the *Sequential Similarity Detection Algorithm (SSDA)* which is probably the most popular representative of the correlation-like matching methods [94]. By means of blur invariants, all templates were placed correctly or almost correctly with a reasonable error 1 pixel. On the other hand, SSDA did not yield satisfactory results. Only the "Island" template was correctly localized because of its distinct structure, while the other templates were misplaced.

We have performed a lot of experiments like this one with various templates, template sizes, blurring masks and noise variance. In a majority of tests, blur invariants gave significantly better results than the SSDA.

Another very frequent task to be solved in remote sensing is *image registration*. Image registration in general is the process of overlaying two or more images of the same scene acquired from different viewpoints, by different sensors and/or at different times so that the pixels of the same coordinates in the images correspond to the same part of the scene. Image registration is required as a pre-processing stage in analysis of remotely sensed data, medical image analysis, image fusion, in automatic change detection and scene monitoring, among others.

Regardless of the image data involved and of the particular application, image registration usually consists of the four major steps.

First, control points (CPs) are detected both in the reference and sensed images. Edge intersections, objects centroids or significant contour points can be considered for this purpose. The correspondence between the CP sets in the reference and sensed images

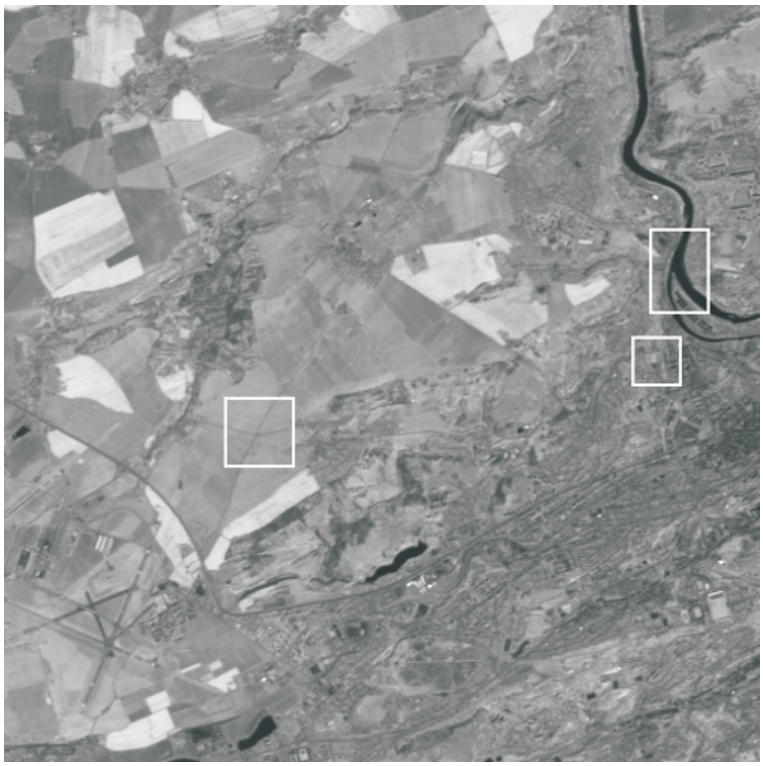

Figure 9: Original $512 \times 512$ SPOT scene (band 3) of the north-western part of Prague, Czech Republic, used for simulation. True locations of the templates are marked.

Figure 10: Simulated AVHRR image ($9 \times 13$ blurring mask + additive noise with STD = 10).

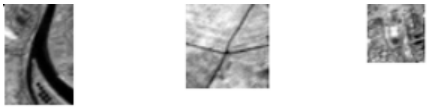

Figure 11: The templates: "Island" (left), "Cross" (middle) and "Stadium" (right).

is then established. Matching methods are based on the image content (cross-correlation, mutual information) or on symbolic description of the CP sets (parameter clustering, graph matching, relaxation). Matching is usually the most difficult part of the registration. After the CP sets have been matched, the type and parameters of spatial transform between the reference and sensed images are estimated. The mapping function can be global or local, depending on the type of the image distortions. Finally, the sensed image is resampled, transformed and overlayed over the reference one.

The invariant functionals can be used in the second step, CP matching. They are calculated over a circular neighborhood of each CP candidate detected earlier. After that, the correspondence is established by minimum distance rule with thresholding in the space of the invariants. Herein described application uses the blur-rotation invariants for registration of satellite images, that are rotated and shifted one another and differently blurred.

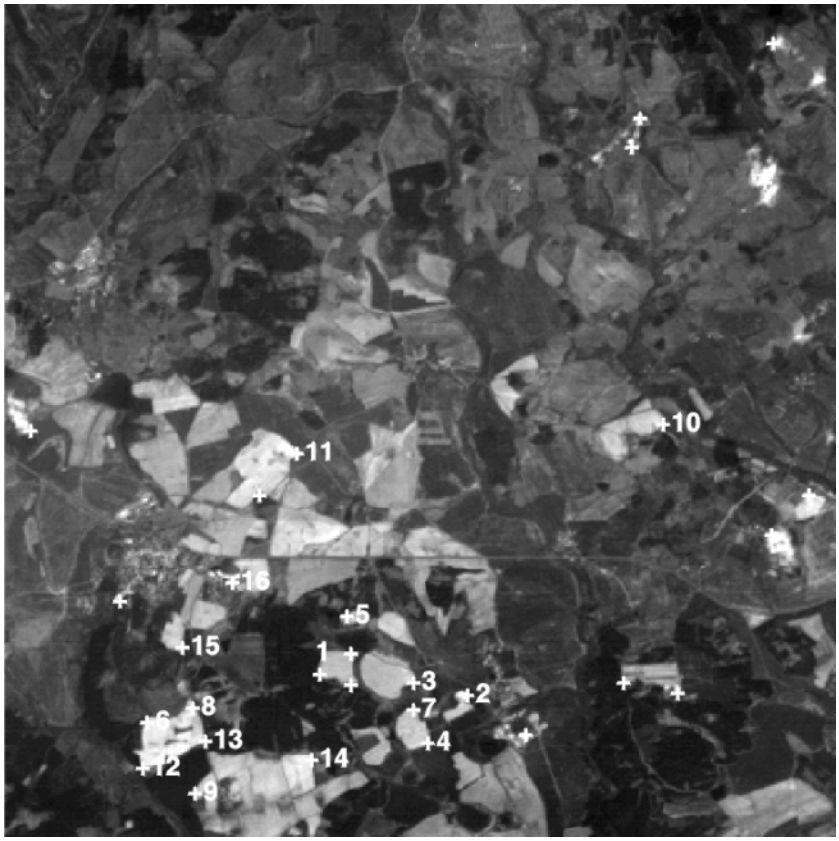


Figure 12: Reference image – SPOT subscene of the size $400 \times 400$ pixels – with the detected control point candidates. Numbered CPCs have their counterparts in the sensed image.

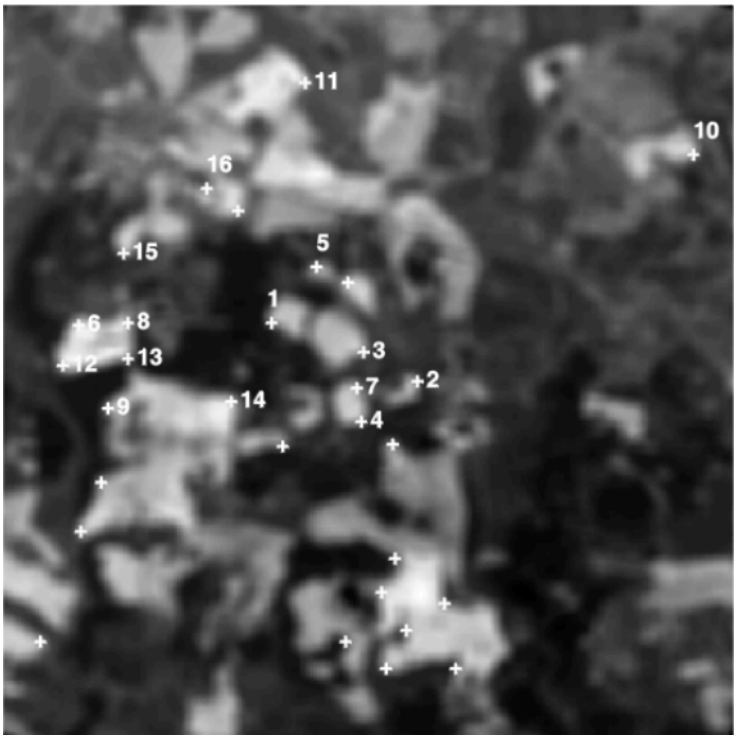


Figure 13: Sensed image – different SPOT subscene of the size $325 \times 325$ pixels, taken during the same flight and covering approximately the same ground – with the control point candidates. The image was rotated by 15 degrees, the nonideal acquisition was simulated by blurring with the $7 \times 7$ uniform square mask. Numbered CPCs have their counterparts in the reference image.

The experiment was performed on real satellite data with simulated blurring. Blurred image simulates a sensor with low spatial resolution. The reference image of the size $400 \times 400$ pixels was extracted from the SPOT subscene, band 2, Czech Republic (see Fig. 12). The sensed image of the size $325 \times 325$ pixels was extracted from the different SPOT subscene, band 2, from the same flight covering approximately the same ground. It was then rotated by 15 degrees and the nonideal acquisition was simulated by blurring with the $7 \times 7$ averaging mask (see Fig. 13). Control point detection and matching was done by similar algorithm to that used in "motion estimation" experiment in the previous section. The sensed image was then transformed using linear mapping function whose coefficients were calculated via least-square method by means of the matched CPs. Inter-pixel gray values were estimated via bilinear interpolation. The co-registered images are shown in Fig. 14. After the registration, any multiframe image processing methods like fusion, multichannel restoration, change detection, and/or multichannel compression can be applied in the overlapped area.

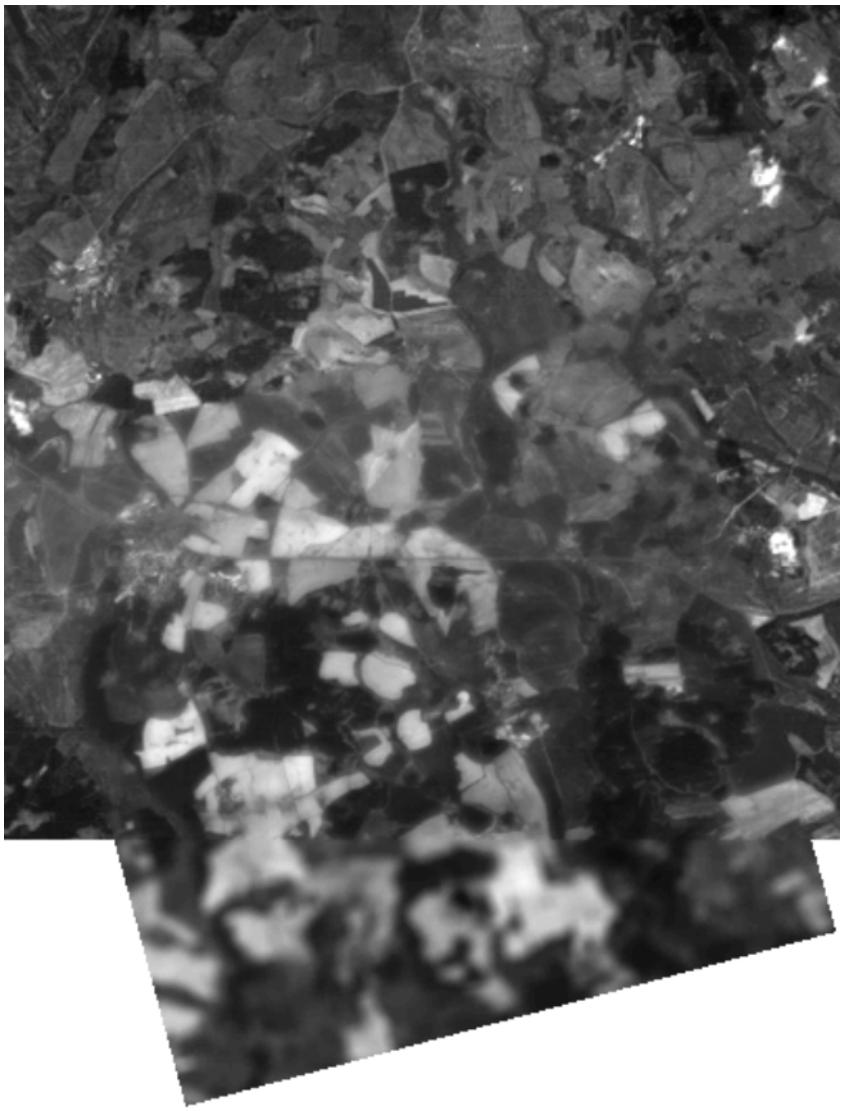

Figure 14: Registered images.

## 10.4 3-D template matching in MRI

Magnetic resonance images are often subject to blurring, namely because limited spatial resolution. In this experiment we show that invariant functionals can be used in template matching.

As a test data, we used a 3-D magnetic resonance image of a human head whose size was $256 \times 256 \times 256$ voxels. Two perpendicular slices are depicted in Fig. 15.

We chose randomly a spherical part of the original MRI image and used it used as a template. The original image was rotated by 30 degrees in all angles, blurred by Gaussian masks of various sizes and corrupted by additive noise of various SNR. The template was shifted across the image and in each its position the invariants of the corresponding part of the image were calculated and compared with the invariants of the template. Thanks

to the rotation invariance of the features, template rotation need not be performed. The "matching position" was localized as that with minimum distance in the space of invariants.

The matching accuracy depends on the SNR (which is obvious) and on the size of the blurring mask. This is because the voxels near the template boundary are affected by the voxels from the outside. This boundary effect of course increases when the blurring becomes larger. One may observe that if the size of the blurring mask is not too large with respect to the size of the template, the results are very good, even if noise is present.

We conducted similar experiment in which we studied the influence of rotation angle and the shape of the blurring masks on the localization error. The MRI image was rotated in all directions by the angle $\alpha$ (where $\alpha = 0, 5, 10, 15, \cdots, 90$, respectively) and blurred by various anisotropic masks. It can be seen from Fig. 16 that even if the rotation is big and the major blurring direction changes, the localization error is still kept reasonably low.

Finally, we extended the matching experiment to more templates. Eight spherical templates of 15-pixel radius were manually extracted from the original MRI data. The original image was then rotated around all three axes by 30 degrees and blurred by anisotropic Gaussian mask with standard deviations [0.5 0.5 0.2]. We looked for the matching position of each template by an exhaustive search within the whole image – no estimation of approximate matching position was used. The results were really encouraging: the positions of five templates were found accurately, in the three other cases the error was one pixel.

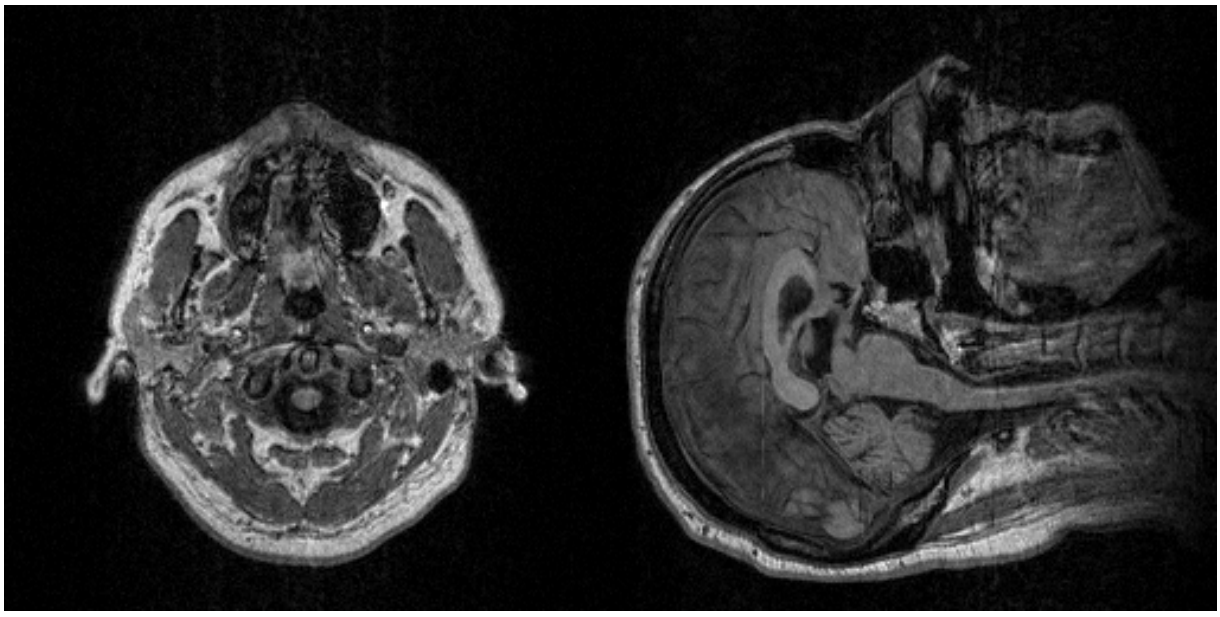

Figure 15: Original MRI data of a human head: 157th axial slice (left) and 130th sagittal slice (right)

The experiments described in this section proved that the proposed invariants can be used successfully in 3-D template matching regardless of rotation and/or blurring of the

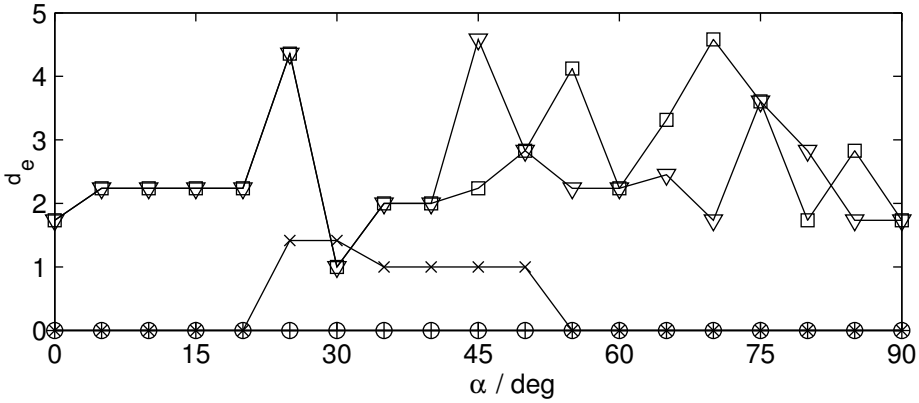


Figure 16: Template matching with anisotropic blurring: $d_e$ – localization error (Euclidean distance from the correct position), $\alpha$ – rotation angle, $\bigcirc$ – no blurring, $\times$ – blurring by $1 \times 1 \times 3$ mask after rotation, $+$ – blurring by $1 \times 1 \times 3$ mask before rotation, $\square$ – blurring by $3 \times 3 \times 5$ mask after rotation, $\bigtriangledown$ – blurring by $3 \times 3 \times 5$ mask before rotation.

images involved. There are, however, some limitations posed mainly by boundary effect and, of course, by noise if it is heavy. In all these experiments we were using six invariants only. The results can be further improved by employing more invariants but the higher the order the less robustness of the respective moments.

# 11 Conclusion

This tutorial presented a review of moment-based invariant functionals, their history, basic principles, and methods how to construct them. We demonstrated that invariant functionals can be used in image analysis as features for description and recognition of objects in degraded images.

Invariant-based approach is a significant step towards robust and reliable object recognition methods. It has a deep practical impact because many pattern recognition problems would not be solvable otherwise. In practice, image acquisition is always degraded by unrecoverable errors and the knowledge of invariants with respect to these errors is a crucial point. This observation should influence future research directions and should be also incorporated in the education.

In the future research, a very promising topic are pseudo invariants. It has not been done much work on pseudo invariants but common belief is that they perform a way how to break the limitations of invariants. While the invariants must be by their definition constant within a class, pseudo invariants are allowed to change "slightly". This gives a chance to increase discrimination power because invariants which are invariant with respect to many factors usually suffer by lack of discriminability.

# References


[1] D. Hilbert, *Theory of Algebraic Invariants*. Cambridge University Press, 1993.

[2] G. B. Gurevich, *Foundations of the Theory of Algebraic Invariants*. Groningen, The Netherlands: Nordhoff, 1964.

[3] I. Schur, *Vorlesungen uber Invariantentheorie*. Berlin: Springer, 1968.

[4] M. K. Hu, "Visual pattern recognition by moment invariants," *IRE Trans. Information Theory*, vol. 8, pp. 179–187, 1962.

[5] S. A. Dudani, K. J. Breeding, and R. B. McGhee, "Aircraft identification by moment invariants," *IEEE Trans. Computers*, vol. 26, pp. 39–45, 1977.

[6] S. O. Belkasim, M. Shridhar, and M. Ahmadi, "Pattern recognition with moment invariants: a comparative study and new results," *Pattern Recognition*, vol. 24, pp. 1117–1138, 1991.

[7] R. Y. Wong and E. L. Hall, "Scene matching with invariant moments," *Computer Graphics and Image Processing*, vol. 8, pp. 16–24, 1978.

[8] A. Goshtasby, "Template matching in rotated images," *IEEE Trans. Pattern Analysis and Machine Intelligence*, vol. 7, pp. 338–344, 1985.

[9] J. Flusser and T. Suk, "A moment-based approach to registration of images with affine geometric distortion," *IEEE Trans. Geoscience and Remote Sensing*, vol. 32, pp. 382–387, 1994.

[10] R. Mukundan and K. R. Ramakrishnan, "An iterative solution for object pose parameters using image moments," *Pattern Recognition Letters*, vol. 17, pp. 1279–1284, 1996.

[11] R. Mukundan and N. K. Malik, "Attitude estimation using moment invariants," *Pattern Recognition Letters*, vol. 14, pp. 199–205, 1993.

[12] A. Sluzek, "Identification and inspection of 2-D objects using new moment-based shape descriptors," *Pattern Recognition Letters*, vol. 16, pp. 687–697, 1995.

[13] F. El-Khaly and M. A. Sid-Ahmed, "Machine recognition of optically captured machine printed arabic text," *Pattern Recognition*, vol. 23, pp. 1207–1214, 1990.

[14] K. Tsirikolias and B. G. Mertzios, "Statistical pattern recognition using efficient two-dimensional moments with applications to character recognition," *Pattern Recognition*, vol. 26, pp. 877–882, 1993.

[15] A. Khotanzad and Y. H. Hong, "Invariant image recognition by Zernike moments," *IEEE Trans. Pattern Analysis and Machine Intelligence*, vol. 12, pp. 489–497, 1990.

[16] J. Flusser and T. Suk, "Affine moment invariants: A new tool for character recognition," *Pattern Recognition Letters*, vol. 15, pp. 433–436, 1994.

[17] S. Maitra, "Moment invariants," *Proc. of the IEEE*, vol. 67, pp. 697–699, 1979.

[18] T. M. Hupkens and J. de Clippeleir, "Noise and intensity invariant moments," *Pattern Recognition*, vol. 16, pp. 371–376, 1995.

[19] L. Wang and G. Healey, "Using Zernike moments for the illumination and geometry invariant classification of multispectral texture," *IEEE Trans. Image Processing*, vol. 7, pp. 196–203, 1998.

[20] Y. Li, "Reforming the theory of invariant moments for pattern recognition," *Pattern Recognition*, vol. 25, pp. 723–730, 1992.

[21] W. H. Wong, W. C. Siu, and K. M. Lam, "Generation of moment invariants and their uses for character recognition," *Pattern Recognition Letters*, vol. 16, pp. 115–123, 1995.

[22] J. Flusser, "On the independence of rotation moment invariants," *Pattern Recognition*, vol. 33, pp. 1405-1410, 2000.

[23] J. Flusser, "On the inverse problem of rotation moment invariants," *Pattern Recognition*, vol. 35, pp. 3015-3017, 2002.

[24] M. R. Teague, "Image analysis via the general theory of moments," *J. Optical Soc. of America*, vol. 70, pp. 920–930, 1980.

[25] A. Wallin and O. Kubler, "Complete sets of complex Zernike moment invariants and the role of the pseudoinvariants," *IEEE Trans. Pattern Analysis and Machine Intelligence*, vol. 17, pp. 1106–1110, 1995.

[26] J. Flusser and T. Suk, "Pattern recognition by affine moment invariants," *Pattern Recognition*, vol. 26, pp. 167–174, 1993.

[27] T. H. Reiss, "The revised fundamental theorem of moment invariants," *IEEE Trans. Pattern Analysis and Machine Intelligence*, vol. 13, pp. 830–834, 1991.

[28] R. J. Prokop and A. P. Reeves, "A survey of moment-based techniques for unoccluded object representation and recognition," *CVGIP: Graphical Models and Image Processing*, vol. 54, pp. 438–460, 1992.

[29] C. H. Teh and R. T. Chin, "On image analysis by the method of moments," *IEEE Trans. Pattern Analysis and Machine Intelligence*, vol. 10, pp. 496–513, 1988.

[30] Y. S. Abu-Mostafa and D. Psaltis, "Recognitive aspects of moment invariants," *IEEE Trans. Pattern Analysis and Machine Intelligence*, vol. 6, pp. 698–706, 1984.

[31] S. X. Liao and M. Pawlak, "On image analysis by moments," *IEEE Trans. Pattern Analysis and Machine Intelligence*, vol. 18, pp. 254–266, 1996.

[32] M. Pawlak, "On the reconstruction aspects of moment descriptors," *IEEE Trans. Information Theory*, vol. 38, pp. 1698–1708, 1992.

[33] R. R. Bailey and M. Srinath, "Orthogonal moment features for use with parametric and non-parametric classifiers," *IEEE Trans. Pattern Analysis and Machine Intelligence*, vol. 18, pp. 389–398, 1996.

[34] Y. S. Abu-Mostafa and D. Psaltis, "Image normalization by complex moments," *IEEE Trans. Pattern Analysis and Machine Intelligence*, vol. 7, pp. 46–55, 1985.

[35] M. Gruber and K. Y. Hsu, "Moment-based image mormalization with high noise-tolerance," *Pattern Recognition*, vol. 19, pp. 136–139, 1997.

[36] L. Yang and F. Albregtsen, "Fast and exact computation of cartesian geometric moments using discrete Green's theorem," *Pattern Recognition*, vol. 29, pp. 1061–1073, 1996.

[37] L. van Gool, T. Moons, and D. Ungureanu, "Affine/photometric invariants for planar intensity patterns," in *Proc. 4th ECCV'96*, vol. LNCS 1064, pp. 642–651, Springer, 1996.

[38] F. Mindru, T. Moons, and L. van Gool, "Recognizing color patterns irrespective of viewpoint and illumination," in *Proc. IEEE Conf. Computer Vision Pattern Recognition CVPR'99*, vol. 1, pp. 368–373, 1999.

[39] J. Flusser and T. Suk, "Degraded image analysis: An invariant approach," *IEEE Trans. Pattern Analysis and Machine Intelligence*, vol. 20, no. 6, pp. 590–603, 1998.

[40] J. Flusser, T. Suk, and S. Saic, "Recognition of blurred images by the method of moments," *IEEE Trans. Image Processing*, vol. 5, pp. 533–538, 1996.

[41] Y. Zhang, C. Wen, and Y. Zhang, "Estimation of motion parameters from blurred images," *Pattern Recognition Letters*, vol. 21, pp. 425–433, 2000.

[42] Y. Zhang, C. Wen, Y. Zhang, and Y. Soh, "Determination of blur and affine combined invariants by normalization," *Pattern Recognition*, vol. 35, pp. 211–221, 2002.

[43] J. Lu and Y. Yoshida, "Blurred image recognition based on phase invariants," *IEICE Trans. Fundamentals of El. Comm. and Comp. Sci.*, vol. E82A, pp. 1450–1455, 1999.

[44] Y. Bentoutou, N. Taleb, M. Mezouar, M. Taleb, and L. Jetto, "An invariant approach for image registration in digital subtraction angiography," *Pattern Recognition*, vol. 35, pp. 2853–2865, 2002.

[45] Y. Zhang, Y. Zhang, and C. Wen, "A new focus measure method using moments," *Image and Vision Computing*, vol. 18, pp. 959–965, 2000.

[46] J. Flusser, T. Suk, and S. Saic, "Image features invariant with respect to blur," *Pattern Recognition*, vol. 28, pp. 1723–1732, 1995.

[47] J. Flusser, T. Suk, and S. Saic, "Recognition of images degraded by linear motion blur without restoration," *Computing Suppl.*, vol. 11, pp. 37–51, 1996.

[48] A. Stern, I. Kruchakov, E. Yoavi, and S. Kopeika, "Recognition of motion-blured images by use of the method of moments," *Applied Optics*, vol. 41, pp. 2164-2172, 2002.

[49] J. Flusser and B. Zitová, "Combined invariants to linear filtering and rotation," *Int'l. Journal of Pattern Recognition and Artificial Intelligence*, vol. 13, no. 8, pp. 1123–1136, 1999.

[50] T. Suk and J. Flusser, "Combined blur and affine moment invariants and their use in pattern recognition," *Pattern Recognition*, vol. 36, pp. 2895–2907, 2003.

[51] J. Flusser, B. Zitová, and T. Suk, "Invariant-based registration of rotated and blurred images," in *IEEE 1999 International Geoscience and Remote Sensing Symposium. Proceedings* (I. S. Tammy, ed.), (Los Alamitos), pp. 1262–1264, IEEE Computer Society, June 1999.

[52] B. Zitová and J. Flusser, "Estimation of camera planar motion from defocused images," in *Proc. IEEE Int'l. Conf. Image Proc ICIP'02*, vol. II, pp. 329-332, Rochester, NY, September 2002.

[53] F. A. Sadjadi and E. L. Hall, "Three dimensional moment invariants," *IEEE Trans. Pattern Analysis and Machine Intelligence*, vol. 2, pp. 127–136, 1980.

[54] C. H. Lo and H. S. Don, "3-D moment forms: Their construction and application to object identification and positioning," *IEEE Trans. Pattern Analysis and Machine Intelligence*, vol. 11, pp. 1053–1064, 1989.

[55] X. Guo, "3-D moment invariants under rigid transformation," in *Proc. 5th Int'l. Conf. CAIP'93*, vol. LNCS 719, pp. 518–522, Springer, Budapest, Hungary, 1993.

[56] J. M. Galvez and M. Canton, "Normalization and shape recognition of three dimensional objects by 3-D moments," *Pattern Recognition*, vol. 26, pp. 667–681, 1993.

[57] T. H. Reiss, "Features invariant to linear transformations in 2D and 3D," in *Proc. 11th Int'l. Conf. Pattern Recognition ICPR'92*, vol. III, pp. 493–496, IEEE Computer Society Press, Hague, The Netherlands, 1992.

[58] G. Taubin and D. B. Cooper, "Object recognition based on moment (or algebraic) invariants," in *Geometric Invariance in Computer Vision* (J. L. Mundy and A. Zisserman, eds.), pp. 375–397, MIT Press, 1992.

[59] V. Markandey and R. J. P. de Figueiredo, "Robot sensing techniques based on hogh-dimensional moment invariants and tensors," *IEEE Trans. Robotics and Automation*, vol. 8, pp. 186–195, 1992.

[60] A. G. Mamistvalov, "On the fundamental theorem of moment invariants," *Bull. Acad. Sci. Georgian SSR*, vol. 59, pp. 297–300, 1970 (in Russian).

[61] A. G. Mamistvalov, "$n$-dimensional moment invariants and conceptual mathematical theory of recognition $n$-dimensional solids," *IEEE Trans. Pattern Analysis and Machine Intelligence*, vol. 20, pp. 819–831, 1998.

[62] A. G. Mamistvalov, "On the construction of affine invariants of $n$-dimensional patterns," *Bull. Acad. Sci. Georgian SSR*, vol. 76, pp. 61–64, 1974 (in Russian).

[63] J. Flusser, J. Boldyš, and B. Zitová, "Invariants to convolution in arbitrary dimensions," *Journal of of Mathematical Imaging and Vision*, vol. 13, pp. 101–113, 2000.

[64] J. Flusser, J. Boldyš, and B. Zitová, "Moment forms invariant to rotation and blur in arbitrary number of dimensions," *IEEE Transactions on Pattern Analysis and Machine Intelligence*, vol. 25, no. 2, pp. 234–246, 2003.

[65] J. Flusser and T. Suk, "Pattern Recognition by Means of Affine Moment Invariants," Tech. Rep. 1726, ÚTIA AV ČR, Praha, 1991.

[66] L. Van Gool, T. Moons, E. Pauwels, and A. Oosterlinck, "Vision and Lie's approach to invariance," *Image and Vision Computing* vol. 13 pp. 259–277, 1995.

[67] T. Suk and J. Flusser, " Projective Moment Invariants," *IEEE Trans. Pattern Anal. Mach. Intell.*, submitted in 2003.

[68] T. Suk and J. Flusser, "Graph method for generating affine moment invariants," *Int'l. Conf. Pattern Recognition ICPR'04*, Cambridge, U.K., August 2004 (submitted).

[69] M. I. Sezan and A. M. Tekalp, "Survey of recent developments in digital image restoration," *Optical Engineering*, vol. 29, pp. 393–404, 1990.

[70] D. Kundur and D. Hatzinakos, "Blind image deconvolution," *IEEE Signal Processing Magazine*, vol. 13, no. 3, pp. 43–64, 1996.

[71] R. Mukundan and K. R. ramakrishnan, *Moment Functions in Image Analysis*. World Scientific, Singapore, 1998.

[72] M. F. Zakaria, L. J. Vroomen, P. Zsombor-Murray, and J. M. van Kessel, "Fast algorithm for the computation of moment invariants," *Pattern Recognition*, vol. 20, pp. 639–643, 1987.

[73] M. Dai, P. Baylou, and M. Najim, "An efficient algorithm for computation of shape moments from run-length codes or chain codes," *Pattern Recognition*, vol. 25, pp. 1119–1128, 1992.

[74] B. C. Li, "A new computation of geometric moments," *Pattern Recognition*, vol. 26, pp. 109–113, 1993.

[75] I. M. Spiliotis and B. G. Mertzios, "Real-time computation of two-dimensional moments on binary images using image block representation," *IEEE Trans. Image Processing*, vol. 7, pp. 1609–1615, 1998.

[76] J. Flusser, "Refined moment calculation using image block representation," *IEEE Trans. Image Processing*, vol. 9, pp. 1977-1978, 2000.

[77] H. Sossa, C. Yañez and J. L. Díaz, "Computing geometric moments using morphological erosions," *Pattern Recognition*, vol. 34, pp. 271-276, 2001.

[78] "A new computation of shape moments via quadtree decomposition," *Pattern Recognition*, vol. 34, pp. 1319–1330, 2001.

[79] B. C. Li and J. Shen, "Fast computation of moment invariants," *Pattern Recognition*, vol. 24, pp. 807–813, 1991.

[80] X. Y. Jiang and H. Bunke, "Simple and fast computation of moments," *Pattern Recognition*, vol. 24, pp. 801–806, 1991.

[81] W. Philips, "A new fast algorithm for moment computation," *Pattern Recognition*, vol. 26, pp. 1619–1621, 1993.

[82] J. G. Leu, "Computing a shape's moments from its boundary," *Pattern Recognition*, vol. 24, pp. 949–957, 1991.

[83] M. H. Singer, "A general approach to moment calculation for polygons and line segments," *Pattern Recognition*, vol. 26, pp. 1019–1028, 1993.

[84] K. Chen, "Efficient parallel algorithms for the computation of two-dimensional image moments," *Pattern Recognition*, vol. 23, pp. 109–119, 1990.

[85] K. L. Chung, "Computing horizontal/vertical convex shape's moments on reconfigurable meshes," *Pattern Recognition*, vol. 29, pp. 1713–1717, 1996.

[86] W. G. Lin and S. Wang, "A note on the calculation of moments," *Pattern Recognition Letters*, vol. 15, pp. 1065–1070, 1994.

[87] B. C. Li, "The moment calculation of polyhedra," *Pattern Recognition*, vol. 26, pp. 1229–1233, 1993.

[88] B. C. Li and S. D. Ma, "Efficient computation of 3D moments," *Proc. 12th Int. Conf. Pattern Recognition*, vol. I, pp. 22–26, Jerusalem, 1994.

[89] L. Yang, F. Albregtsen, and T. Taxt, "Fast computation of 3-D geometric moments using a discrete divergence theorem and a generalization to higher dimensions," *Graphical Models and Image Processing*, vol. 59, pp. 97–108, 1997.

[90] B. Zitová, J. Kautsky, G. Peters, and J. Flusser, "Robust detection of significant points in multiframe images," *Pattern Recognition Letters*, vol. 20, pp. 199–206, 1999.

[91] J. Flusser, "Object matching by means of matching likelihood coefficients," *Pattern Recognition Letters*, vol. 16, pp. 893–900, 1995.

[92] B. Zitová and J. Flusser, "Image registration methods: A survey," *Image and Vision Computing*, vol. 21, pp. 977–1000, 2003.

[93] S. E. Reichenbach, D. E. Koehler, and D. W. Strelow, "Restoration and reconstruction of AVHRR images," *IEEE Trans. Geoscience and Remote Sensing*, vol. 33, pp. 997–1007, 1995.

[94] D. I. Barnea and H. F. Silverman, "A class of algorithms for fast digital registration," *IEEE Trans. Computers*, vol. 21, pp. 179–186, 1972.